Mean full-depth summer circulation and transports at the northern periphery of the Atlantic Ocean in the 2000s

Artem Sarafanov,[1] Anastasia Falina,[1] Herlé Mercier,[2] Alexey Sokov,[1] Pascale Lherminier,[2] Claire Gourcuff,[2] Sergey Gladyshev,[1] Fabienne Gaillard,[2] and Nathalie Daniault[3]

Received 7 September 2011; revised 4 November 2011; accepted 8 November 2011; published 24 January 2012.

[1] A mean state of the full-depth summer circulation in the Atlantic Ocean in the region in between Cape Farewell (Greenland), Scotland and the Greenland-Scotland Ridge (GSR) is assessed by combining 2002–2008 yearly hydrographic measurements at 59.5°N, mean dynamic topography, satellite altimetry data and available estimates of the Atlantic–Nordic Seas exchange. The mean absolute transports by the upper-ocean, mid-depth and deep currents and the Meridional Overturning Circulation (MOCσ = 16.5 ± 2.2 Sv, at σ_0 = 27.55) at 59.5°N are quantified in the density space. Inter-basin and diapycnal volume fluxes in between the 59.5°N section and the GSR are then estimated from a box model. The dominant components of the meridional exchange across 59.5°N are the North Atlantic Current (NAC, 15.5 ± 0.8 Sv, σ_0 < 27.55) east of the Reykjanes Ridge, the northward Irminger Current (IC, 12.0 ± 3.0 Sv) and southward Western Boundary Current (WBC, 32.1 ± 5.9 Sv) in the Irminger Sea and the deep water export from the northern Iceland Basin (3.7 ± 0.8 Sv, σ_0 > 27.80). About 60% (12.7 ± 1.4 Sv) of waters carried in the MOCσ upper limb (σ_0 < 27.55) by the NAC/IC across 59.5°N (21.1 ± 1.0 Sv) recirculates westward south of the GSR and feeds the WBC. 80% (10.2 ± 1.7 Sv) of the recirculating NAC/IC-derived upper-ocean waters gains density of σ_0 > 27.55 and contributes to the MOCσ lower limb. Accordingly, the contribution of light-to-dense water conversion south of the GSR (∼10 Sv) to the MOCσ lower limb at 59.5°N is one and a half times larger than the contribution of dense water production in the Nordic Seas (∼6 Sv).

Citation: Sarafanov A., A. Falina, H. Mercier, A. Sokov, P. Lherminier, C. Gourcuff, S. Gladyshev, F. Gaillard, and N. Daniault (2012), Mean full-depth summer circulation and transports at the northern periphery of the Atlantic Ocean in the 2000s, *J. Geophys. Res.*, *117*, C01014, doi:10.1029/2011JC007572.

1. Introduction

[2] The large-scale oceanic circulation in the North Atlantic is an important element of the climate system. Warm saline upper-ocean waters transported by the North Atlantic Current from the subtropics release heat to the atmosphere, gain density due to cooling, mix with cold fresh Arctic-origin waters and eventually sink in the subpolar basins and Nordic Seas thereby generating the return equatorward flow of colder fresher waters at depths. This circulation pattern, known as the Atlantic Meridional Overturning Circulation (MOC), is one of the principal contributors to the meridional heat transport and the Earth's freshwater cycle.

[3] Progress in understanding the Atlantic MOC spatial structure, variability and driving mechanisms requires observation-based estimates of transports in the whole system of Atlantic currents contributing to the meridional exchange. Observation-derived transports are also needed as benchmarks for numerical models. Although the ocean observing system has been developed fast in the past decades, such estimates are still not numerous [see *Garzoli et al.*, 2009; *Cunningham et al.*, 2009; *Rhein et al.*, 2011]. The aim of the present study is to improve the situation by providing an estimate of the 2002–2008 mean summer circulation in the northern North Atlantic in the region in between Cape Farewell (Greenland), Scotland and the Greenland-Scotland Ridge (Figure 1).

[4] Transports concentrated in 'narrow sites', such as the passages between Greenland, Iceland and Scotland, and at the western boundary of the North Atlantic can be efficiently measured with moored current meters. This is where sustained observations have primarily been made [e.g., *Macrander et al.*, 2005; *Østerhus et al.*, 2005, 2008; *Dickson et al.*, 2008; *Bacon and Saunders*, 2010; *Fischer et al.*, 2010; *Daniault et al.*, 2011a], providing reliable estimates of time-mean transports of the currents and their variability.

[5] Quantification of full-depth basin-wide spatial distribution of transports in the vast ocean interior is a more challenging task. The only effective tool for carrying out this task

[1]P.P. Shirshov Institute of Oceanology, Moscow, Russia.
[2]Laboratoire de Physique des Océans, UMR 6523, Ifremer, CNRS/IRD/UBO, Plouzane, France.
[3]Laboratoire de Physique des Océans, UMR 6523, UBO, CNRS/IFREMER/IRD, Brest, France.

0148-0227/12/2011JC007572

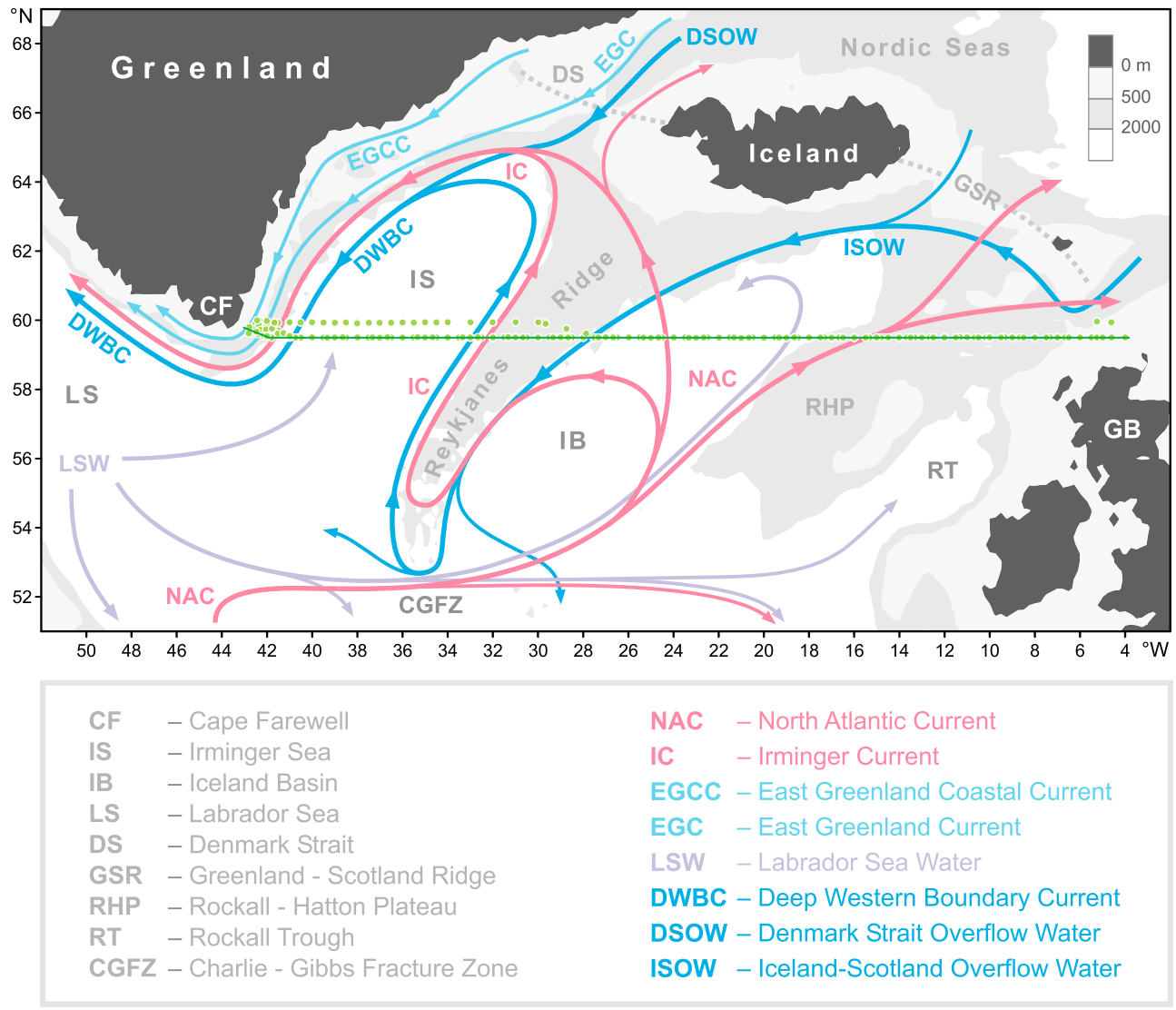

Figure 1. Schematic diagram of the large-scale circulation in the northern North Atlantic compiled from *Schmitz and McCartney* [1993], *Schott and Brandt* [2007, Plate 1], *Sutherland and Pickart* [2008, Figure 16] and *Lherminier et al.* [2010, Figure 1b]. Abbreviations for the main topographic features, currents and water masses are explained in the legend. The nominal location of the 59.5°N Greenland to Scotland section is shown with the solid green line. Light green circles indicate the locations of the CTD stations carried out in the 7 yearly surveys in 2002–2008. Table 1 lists the hydrographic cruises.

is ship-based hydrographic/velocity measurements at trans-oceanic sections, providing information on 'instantaneous' (synoptic) transport structure in the entire water column and on the MOC intensity at time of measurements.

[6] Available estimates of the large-scale circulation in the northern North Atlantic between Cape Farewell and the European coast are based on hydrographic/ADCP data from six transatlantic surveys conducted in 1991–2006 [see *Bersch*, 1995; *Bacon*, 1997; *Lherminier et al.*, 2007, 2010; *Gourcuff et al.*, 2011]. While being an essential source of information on the synoptic circulation states, these observations are not frequent enough (several sections for one and a half decade) to efficiently resolve variability occurring on a variety of time scales: from weekly to decadal.

[7] The problem is illustrated in Figure 2, where we compiled available estimates of the surface-to-bottom transport of the Western Boundary Current (WBC) at Cape Farewell. The extent of the WBC transport variability is striking. Given the associated uncertainties, transports in the upper (EGIC (East Greenland/Irminger Current), $\sigma_0 < 27.80$) and lower (DWBC (Deep Western Boundary Current),

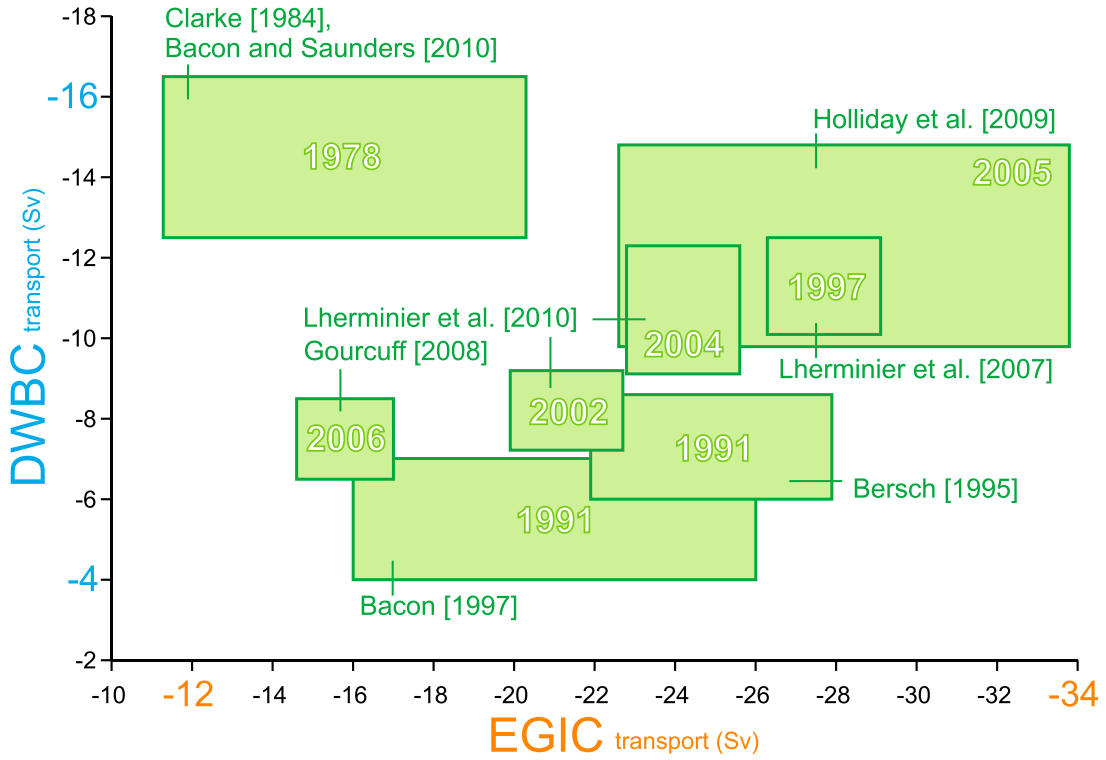

Figure 2. Summary of the available estimates of the top-to-bottom transport (Sv) in the Western Boundary Current (WBC) system at Cape Farewell as obtained by combining hydrographic and direct velocity measurements. For each estimate, the Deep Western Boundary Current transport (DWBC, $\sigma_0 > 27.80$) is plotted versus the East Greenland/Irminger Current transport (EGIC, $\sigma_0 < 27.80$). The lengths of the rectangle's sides correspond to the uncertainties in the DWBC and EGIC transport estimates. Based on the transports from April 1978 [*Clarke*, 1984; *Bacon and Saunders*, 2010], September 1991 [*Bersch*, 1995], August 1991 [*Bacon*, 1997], September 1997 [*Lherminier et al.*, 2007], June 2002 and 2004 [*Lherminier et al.*, 2010], August–September 2005 [*Holliday et al.*, 2009] and June 2006 [*Gourcuff*, 2008].

$\sigma_0 > 27.80$) parts of the WBC vary in the 12–34 Sv and 4–16 Sv ranges, respectively (1 Sv = 10^6 m^3 s^{-1}). Noteworthy, the latter range is close to the peak-to-peak amplitude in the ~10 month long record of the DWBC transport obtained by *Bacon and Saunders* [2010] from mooring data. Clearly, a single estimate (in particular, the widely quoted one by *Clarke* [1984]) should not be regarded as a typical value for the WBC transport. The mean WBC = EGIC + DWBC transport in the 2000s is of about 32 = 22 + 10 Sv, with the caveat that the mean derived from the few widely scattered estimates is far from being robust. The WBC is the best-observed current in the region; 'direct' estimates of the MOC and transports of the open-ocean currents are scarcer.

[8] Thus, the available transport estimates built solely upon ship-based measurements are not enough alone to extract reliable information on climate-relevant low-frequency changes in the basin-wide circulation or its reference mean state. Complementary data and approaches are needed.

[9] Since the early 1990s, continuous satellite altimetry missions have provided data on the sea-surface height anomalies and, hence, information on the short-term to decadal variability of the sea-surface geostrophic currents. The use of altimetry data in different combinations with repeat hydrography, direct current measurements, drifter/float data and mean dynamic topography (MDT) led to a substantial progress in studying the variability of the North Atlantic subpolar gyre surface circulation [*Häkkinen and Rhines*, 2004, 2009], the Atlantic MOC [*Willis*, 2010], the WBC [*Sarafanov et al.*, 2010; *Våge et al.*, 2011; *Daniault et al.*, 2011b], the full-depth circulation in the southern Irminger Sea [*Våge et al.*, 2011] and the Atlantic inflow to the Nordic Seas [*Mork and Skagseth*, 2010].

[10] In the present study, we employ altimetry data in a combination with MDT and repeat hydrography to quantify the 2002–2008 mean summer circulation across 59.5°N in the North Atlantic. We take the following advantage of altimetry: averaging of the altimetry-derived sea-surface velocity (v) anomalies over time efficiently filters out high-frequency variability, e.g., the 'noise' associated with eddies. A combination of thus obtained time-mean sea-surface v anomalies with the sea-surface v derived from MDT allows the mean absolute geostrophic velocities at the sea surface to be estimated. This can be done for any time period since the early 1990s for almost the entire World Ocean. However, to 'go beneath' the sea surface (to obtain the mean surface-to-seafloor v profiles required for quantification of the mean full-depth circulation) information on the mean vertical v shears is needed. At 59.5°N in the Atlantic Ocean, this information is available for the 2002–2008 time period owing to the repeat CTD measurements taken in yearly

Table 1. Hydrographic Cruises

Month and Year	Research Vessel	Cruise Number	Principal Investigator
August 2002	*Akademik Mstislav Keldysh*	48	Eugeniy Morozov
June–July 2003	*Akademik Ioffe*	13	Alexey Sokov
June 2004	*Akademik Ioffe*	15	Sergey Pisarev
June 2005	*Akademik Ioffe*	18	Sergey Pisarev
July 2006	*Akademik Ioffe*	21	Alexey Sokov
July 2007	*Akademik Ioffe*	23	Alexey Sokov
June–July 2008	*Akademik Ioffe*	25	Alexey Sokov

summer surveys on board the Russian research vessels (Figure 1 and Table 1).

[11] At the first step, we constructed a full-depth zonal section of the 2002–2008 mean absolute geostrophic v at 59.5°N by referencing the hydrography-derived mean baroclinic v profiles to the mean absolute geostrophic v at the sea surface as derived from altimetry data and MDT. Then, we used the obtained mean v section to assess the MOC intensity and transports by the upper-ocean, mid-depth and deep currents across the section in potential density space. Since our estimates may suffer from possible local and/or large-scale biases in the MDT, a comparison of the derived transports with MDT-independent estimates is essential. Although such estimates are not numerous, the comparison is performed where possible. After making sure that the agreement between our estimates and the available independent ones is very close, we inferred general features of the North Atlantic circulation north of 59.5°N by incorporating existing estimates of the Atlantic–Nordic Seas exchange. The results are presented in the form of schematic circulation diagrams and discussed in the context of the gyre/overturning circulation.

2. What Is the 2002–2008 Mean Circulation State Representative of?

[12] Prior to assessing some mean state of a highly variable phenomenon/system, it is essential to elucidate what this state will be representative of. Indeed, averaging over time might be a useful tool to filter out high-frequency variability ('noise') and to provide a simplified but adequate model of reality in case no substantial qualitative changes occurred in the system during the time span chosen. However, if the system underwent radical changes during the time span, averaging may produce a misleading pattern (e.g., annual mean winds in a monsoon region), a simulacrum [*Baudrillard*, 1988], representative of nothing but itself.

[13] An extreme state of the large-scale circulation in the northern North Atlantic took place in the first half of the 1990s. Strong atmospheric forcing associated with a prolonged period of high North Atlantic Oscillation (NAO) index [*Hurrell*, 1995] (1988–1995, see Figure 3) led to extremely deep convection in the Labrador Sea [*Lazier et al.*, 2002] and, most likely, in the Irminger Sea [*Pickart et al.*, 2003; *Falina et al.*, 2007; *Våge et al.*, 2011]. The deep convection produced large volumes of an exceptionally cold, dense and deep (~1000–2000 m) Labrador Sea Water (LSW) [*Lazier et al.*, 2002; *Yashayaev*, 2007], a weakly stratified water mass transported at the intermediate depths in the subpolar gyre and exported equatorward in the western North Atlantic [*Talley and McCartney*, 1982; *Bower et al.*, 2009]. The intense convection along with strong

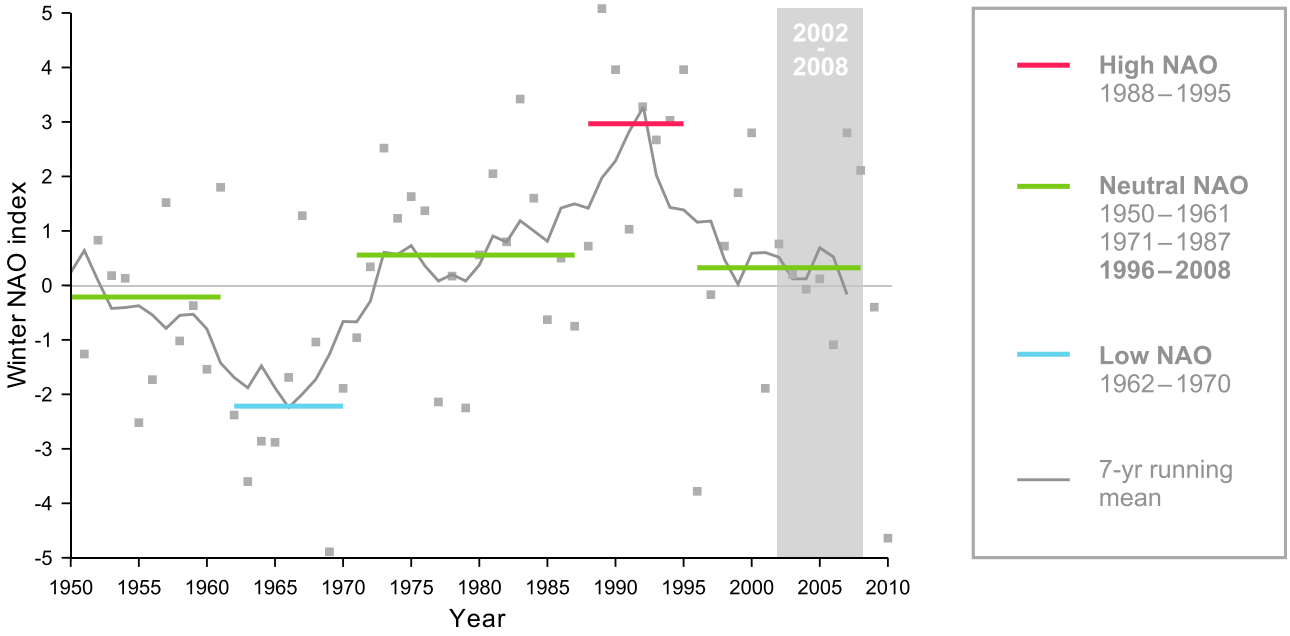

Figure 3. The 1950–2010 time series of the winter (December–March) North Atlantic Oscillation (NAO) index [after *Hurrell*, 1995]. The yearly values and 7-year running mean are shown with the gray dots and gray solid line, respectively. The horizontal color lines denote the mean values for the tentatively identified successive time periods of neutral (1950–1961, 1971–1987, 1996–2008), low (1962–1970) and high (1988–1995) NAO index as explained in the legend. The 2002–2008 time span considered in the present study is marked with the light gray vertical band.

wind-forcing caused strengthening of the subpolar gyre cyclonic circulation [*Häkkinen and Rhines*, 2004, Figure 5c] and eastward expansion of the gyre [*Bersch et al.*, 2007; *Lozier and Stewart*, 2008].

[14] The NAO index dropped in the winter of 1995–1996 and has remained in a neutral phase since then (Figure 3). The associated weakening of the atmospheric forcing resulted in drastic hydrographic and circulation changes in the northern North Atlantic. Weaker convection in the Labrador Sea has produced warmer, lighter and shallower (~500–1200 m) LSW [*Yashayaev*, 2007]. Collapse of the isopycnal dome in the Labrador and Irminger seas due to the drainage of the earlier formed dense LSW [e.g., *Bersch et al.*, 2007], along with weakening of the wind-forcing led to a slowdown [*Häkkinen and Rhines*, 2004, 2009; *Daniault et al.*, 2011b] and contraction [*Hátún et al.*, 2005; *Bersch et al.*, 2007; *Sarafanov et al.*, 2008; *Thierry et al.*, 2008] of the subpolar gyre. The decline of the large-scale cyclonic circulation at the upper levels was accompanied by an intensification of the circulation at deeper levels in the southwestern Labrador Sea [*Dengler et al.*, 2006] and the southern Irminger Sea [*Sarafanov et al.*, 2009, 2010; *Våge et al.*, 2011].

[15] What is particularly important here is that the post-1995 changes described above were relatively fast, and the major qualitative 'shift in the system' occurred by the beginning of the 2000s, i.e., before the 2002–2008 time period considered in the present study. Indeed, the lighter LSW formed after the mid-1990s became a dominant LSW class in the Labrador and Irminger seas by about 2002 [*Yashayaev et al.*, 2007, Figure 1; *van Aken et al.*, 2011, Figure 6], while in the Northeast Atlantic the lagged changes in the LSW layer were much more moderate [*Yashayaev et al.*, 2007, Figure 2; *van Aken et al.*, 2011, Figure 8]. The slowdown of the subpolar gyre cyclonic circulation at the upper levels occurred primarily from the mid-1990s to the early 2000s; the first principal component of the altimetry-derived sea-surface heights in the northern North Atlantic (an index of the subpolar gyre strength [*Häkkinen and Rhines*, 2004]) shows no significant trend after 2002 [*Häkkinen and Rhines*, 2009, Figure 11]. Sustained observations of the WBC at ~53°N and ~56°N near the exit of the Labrador Sea revealed that a notable increase in the alongshore velocity at ~1500 m depth (an indication of the WBC strengthening at the intermediate levels) took place between the mid-late 1990s and the early 2000s [*Dengler et al.*, 2006, Figure 2, section 3]. Similarly, in the southern Irminger Sea near Cape Farewell, a rapid change in the WBC baroclinic structure toward higher velocities at the deep levels occurred in between the mid-1990s and 2000s [*Sarafanov et al.*, 2010]. In the 2000s, the observations of the WBC at Cape Farewell (Figure 2) suggest a coherent transport variability of the upper (EGIC) and lower (DWBC) parts of the WBC. This implies a large contribution to the WBC transport variability in the 2000s by the depth-independent (barotropic) variability that can be efficiently averaged out owing to the altimetry data.

[16] To summarize, the 2002–2008 mean pattern will represent a circulation state 'established' during a prolonged period of relatively weak atmospheric forcing (as manifested by the neutral NAO phase since the second half of the 1990s) foregone by a period of extremely strong forcing (high NAO in the late 1980s to mid-1990s). From this perspective, the 2002–2008 time span is unique over the last several decades (Figure 3). The main characteristic features of the large-scale circulation in the northern North Atlantic in the 2000s are relatively (compared to the early 1990s) (1) weak convection in the Labrador Sea, (2) weak large-scale upper-ocean cyclonic circulation and (3) intensified circulation at the intermediate and deep levels in the Northwest Atlantic.

3. Estimate of the 2002–2008 Mean Summer Transports Across the 59.5°N Section

3.1. Data

[17] The following data sets are used in this study: (1) shipboard full-depth CTD casts from the 2002–2008 yearly repeats of the ~59.5°N transatlantic section [e.g., *Sarafanov et al.*, 2008] (Figure 1 and Table 1); (2) MDT (1/2°) by *Rio and Hernandez* [2004] (hereinafter Rio05 MDT); (3) satellite altimetry-derived sea-surface height anomalies from the weekly AVISO 1/3° gridded topography (http://www.aviso.oceanobs.com/); (4) bathymetry from Etopo2 (1/30°, http://www.ngdc.noaa.gov/mgg/global/etopo2.html); and (5) satellite scatterometry (QuikSCAT) -derived monthly wind stress (1/2°) available from the French ERS Processing and Archiving Facility (http://www.ifremer.fr/cersat/en/data/gridded.htm).

[18] The ~59.5°N section (Figure 1) has been repeated yearly in summer, mostly in June and July, by the Shirshov Institute of Oceanology since 2002 (see Table 1). The data collected in the section have been earlier presented and used for the quantification of the recent thermohaline and circulation changes in the region [e.g., *Falina et al.*, 2007; *Sarafanov et al.*, 2007, 2008, 2009, 2010].

[19] In this study, we used the CTD and oxygen profiles from the 7 repeats of the section carried out in 2002–2008. Nominally, the section runs strictly zonally along the 59.5°N latitude from the Scottish shelf (~4°W) to the East Greenland slope (~42°W), then turns northwestward, crosses the Greenland shelf and ends nearby the southern tip of Greenland (Figure 1). Some CTD casts were made, however, apart the nominal section line. Most notably, in 2002 and 2003, the Irminger Sea was crossed along ~60.0°N. In all such cases, before calculations, the stations were projected along the bottom topography onto the nominal line. A similar technique has recently been substantiated and applied by *Våge et al.* [2011].

3.2. Method

[20] To assess the 2002–2008 mean summer geostrophic circulation and transports across 59.5°N, we constructed a single section of the mean absolute geostrophic v by combining the mean sea-surface v derived from the Rio05 MDT and AVISO sea-surface height anomalies [see *Gourcuff et al.*, 2011] with the mean full-depth v shears derived from the repeat hydrography.

[21] At the first step, the zonal distribution of the 2002–2008 mean summer absolute v of the sea-surface geostrophic flow across the 59.5°N section (Figure 4a) was obtained, with a 1/3° (~18.8 km) resolution corresponding to that of the AVISO data set, as the sum of the MDT-derived v and the 2002–2008 mean summer (May–September) altimetry-derived v anomalies.

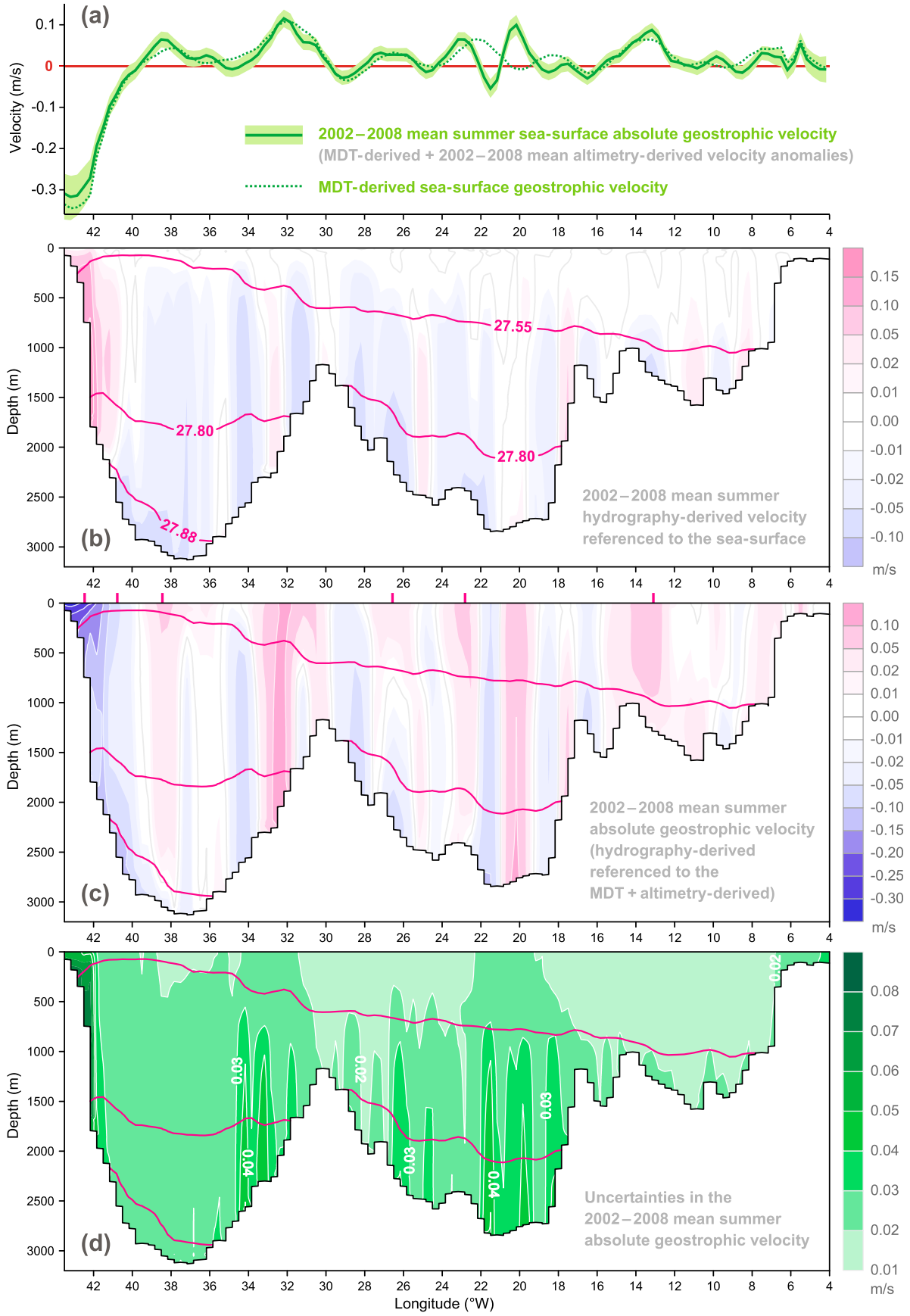
(a)
Velocity (m/s)
2002–2008 mean summer sea-surface absolute geostrophic velocity
(MDT-derived + 2002–2008 mean altimetry-derived velocity anomalies)
MDT-derived sea-surface geostrophic velocity
(b)
Depth (m)
27.55
27.80
27.80
27.88
2002–2008 mean summer
hydrography-derived velocity
referenced to the sea-surface
m/s
(c)
2002–2008 mean summer
absolute geostrophic velocity
(hydrography-derived
referenced to the
MDT + altimetry-derived)
(d)
Uncertainties in the
2002–2008 mean summer
absolute geostrophic velocity
Longitude (°W)

Figure 4

[22] In the next step, we used the CTD data to obtain the full-depth distribution of the mean cross-sectional geostrophic v referenced to the sea surface (Figure 4b). For each of the 7 section repeats, the full-depth profiles of the geostrophic v referenced to the sea surface were calculated for each pair of adjacent stations. Following the approach proposed by *Bacon* [1998, method section], velocities in the so-called 'bottom triangles' were computed by imposing (1) constant v and (2) constant v shear below the deepest common level of the station pair. A single v shear in each triangle was defined as the mean of the two technique outcomes, the difference between which was considered as one of the sources of uncertainty. The sea surface-referenced v thus obtained for each section repeat were then interpolated onto a common 1/3° × 5 m ($\lambda \times$ z, longitude – depth) grid, the zonal dimension of which matches that of the 2002–2008 mean sea-surface v (Figure 4a) obtained by combing the MDT and altimetry data. Then, the 7 grids of the sea surface-referenced v were averaged providing a single pattern of the mean relative v in the water column (Figure 4b). By applying the same gridding-then-averaging procedure to the hydrographic data, the sections of the 2002–2008 mean potential temperature, salinity, potential density (σ_0, density referenced to the sea surface) and oxygen concentrations at 59.5°N (Figure 5) were constructed.

[23] To obtain the full-depth section of the 2002–2008 mean summer absolute geostrophic v across the 59.5°N section (Figure 4c), the hydrography-derived profiles of the mean v referenced to the sea surface (Figure 4b) were adjusted, at each longitude of the 1/3° grid, to the mean sea-surface v derived from the MDT and altimetry (Figure 4a). More specifically, the sought v at each grid node (λ, z) was obtained as the algebraic sum of the mean v (λ, 0) at the sea surface and the mean sea surface-referenced v (λ, z) in the water column. Finally, the 1/3° × 5 m grids of the mean v (Figure 4) and hydrographic properties (Figure 5) were blanked with the Etopo2 bottom topography. The latter was corrected with maximum depths of the CTD casts at 59.5°N (corrected by adding 10 m, a typical distance from the deepest measurement to the bottom), when the casts were deeper than the 'bottom' from Etopo2. Examples of thus obtained v profiles are shown in Figure 6.

[24] The mean absolute geostrophic transport through each of the 1/3° × 5 m grid cells was calculated by multiplying the mean absolute geostrophic v in the cell by the cell area. To account for the contribution of the wind-driven near-surface circulation, the 2002–2008 mean summer Ekman transport across the section (0.5 Sv southward) was calculated from QuikSCAT winds and evenly distributed in the upper 30-m layer [e.g., *Lherminier et al.*, 2010].

[25] When integrating transports over the individual currents and density layers, the zonal and vertical integration limits were defined with zero isotachs (v = 0) and σ_0 isopycnal surfaces, respectively. Unlike synoptic velocity sections, in our estimate, transient energetic mesoscale features, e.g., eddies, are filtered out by averaging over time, and the obtained v field (Figure 4c) is dominated by the prominent mean flows. The zonal limits of the main currents, such as the WBC, Irminger Current and the North Atlantic Current (NAC) branches, are distinguishable in the v field from zero isotachs (Figure 4c), the use of which as the integration limits is thus suitable. In the vertical, the water column was split into three main layers: (1) the upper-ocean layer ($\sigma_0 <$ 27.55) corresponding to the upper limb of the MOCσ (the MOC quantified in σ_0 space [e.g., *Lherminier et al.*, 2007, 2010] (see Figure 7)), (2) the deep water layer ($\sigma_0 >$ 27.80), in which the Nordic Seas overflow-derived waters are transported [e.g., *Dickson and Brown*, 1994], and (3) the mid-depth layer (27.55 $< \sigma_0 <$ 27.80) in between. Additionally, in the Irminger Sea, the deep water transports were quantified for the two sub-layers, 27.80 $< \sigma_0 <$ 27.88 and $\sigma_0 >$ 27.88, which correspond, respectively, to the density classes of the Iceland-Scotland Overflow-derived Water (ISOW, also known as the Northeast Atlantic Deep Water) and the Denmark Strait Overflow Water (DSOW) [e.g., *Holliday et al.*, 2009; *Sarafanov et al.*, 2009]. The integrated transports are shown in Figure 8.

[26] The uncertainties in the mean absolute v (λ, z) (Figure 4d) were calculated, for each grid node, as the square root of the sum of the squared uncertainties in (1) the MDT-derived sea-surface v (λ, 0) [see *Rio and Hernandez*, 2004; *Gourcuff et al.*, 2011], (2) the mean altimetry-derived v (λ, 0) anomalies, and (3) the mean hydrography-derived relative v (λ, z) in the water column. The uncertainties (standard errors) of the mean v (λ, 0) anomalies and of the mean relative v (λ, z) are determined as $\sigma/\sqrt{N-1}$, where σ is the standard deviation and N is the number of statistically independent observations. The standard errors of the mean v (λ, 0) anomalies account for the autocorrelation of the altimetry data [see, e.g., *Sarafanov et al.*, 2010, method section]. The standard errors of the mean hydrography-derived relative v (λ, z) account for the uncertainties associated with the estimation of v (λ, z) in the 'bottom triangles'. This was done by calculating σ (λ, z) from v (λ, z) patterns as obtained by using the two techniques of the v shear extrapolation (i.e., from 14 v patterns in total: 2 patterns for each section repeat), while keeping N = 7. The largest total uncertainties are found above the East Greenland slope at depths of < 2000 m (Figure 4d), where the

Figure 4. On the estimate of the 2002–2008 mean summer absolute geostrophic velocities (v, m s^{-1}) across the 59.5°N transatlantic section. (a) Zonal distribution of the mean absolute v of the sea-surface geostrophic flow across the section (solid green line) as obtained by adding the 2002–2008 mean summer (May–September) altimetry-derived v anomalies to the MDT-derived v (dotted green curve); the associated uncertainties are shown with the light green envelope. (b) The 2002–2008 mean geostrophic v referenced to the sea surface as obtained from the repeat hydrography-derived v shears. (c) The 2002–2008 mean absolute geostrophic v across the 59.5°N section, the algebraic sum of the mean v at the sea surface (Figure 4a) and the mean sea surface-referenced v in the water column (Figure 4b). (d) Uncertainties in the mean absolute geostrophic v. The sign convention is that positive velocities are northward. In Figures 4b–4d, the 2002–2008 mean positions of the σ_0 isopycnals 27.55, 27.80 and, in the Irminger Sea, 27.88 (the upper boundaries of the mid-depth, deep water and DSOW layers, respectively) are overlaid. The magenta ticks at the upper axis in Figure 4c mark the locations of the v profiles shown in Figure 6.

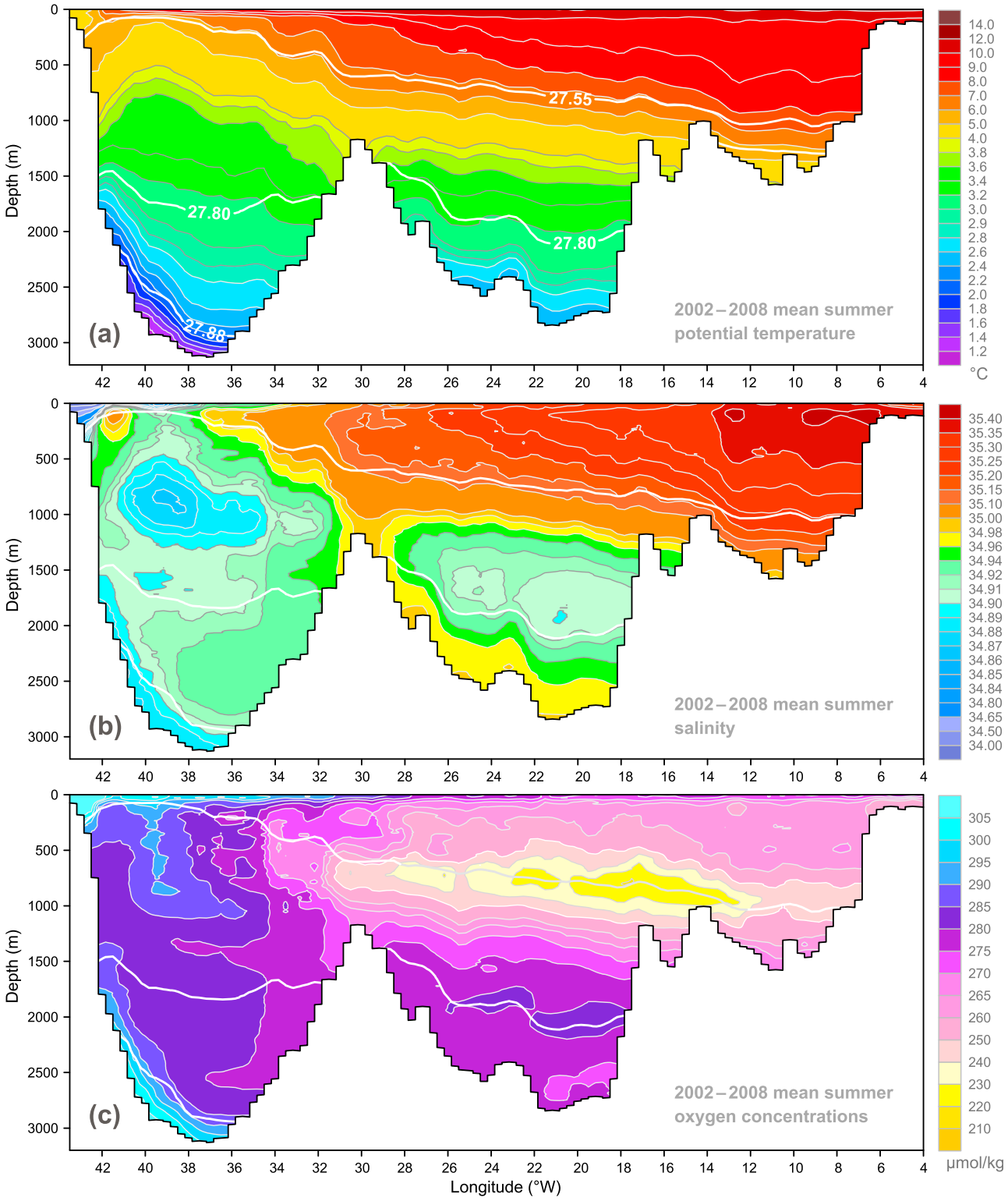

Figure 5. The 2002–2008 mean summer distributions of (a) potential temperature (°C), (b) salinity and (c) oxygen concentrations (μmol kg^{-1}) in the 59.5°N section. The 2002–2008 mean positions of the σ_0 isopycnals 27.55, 27.80 and, in the Irminger Sea, 27.88 are superimposed.

MDT/altimetry-derived mean v (λ, 0) are most uncertain, the hydrography-derived relative v (λ, z) are highly variable, the bathymetry is steep and the bottom triangles are hence typically large.

[27] Based on the obtained uncertainties in the mean v (λ, z) (Figure 4d), the associated uncertainties in the integral transports (see Figure 8) were estimated by propagation of the transport uncertainties in individual grid cells. Since

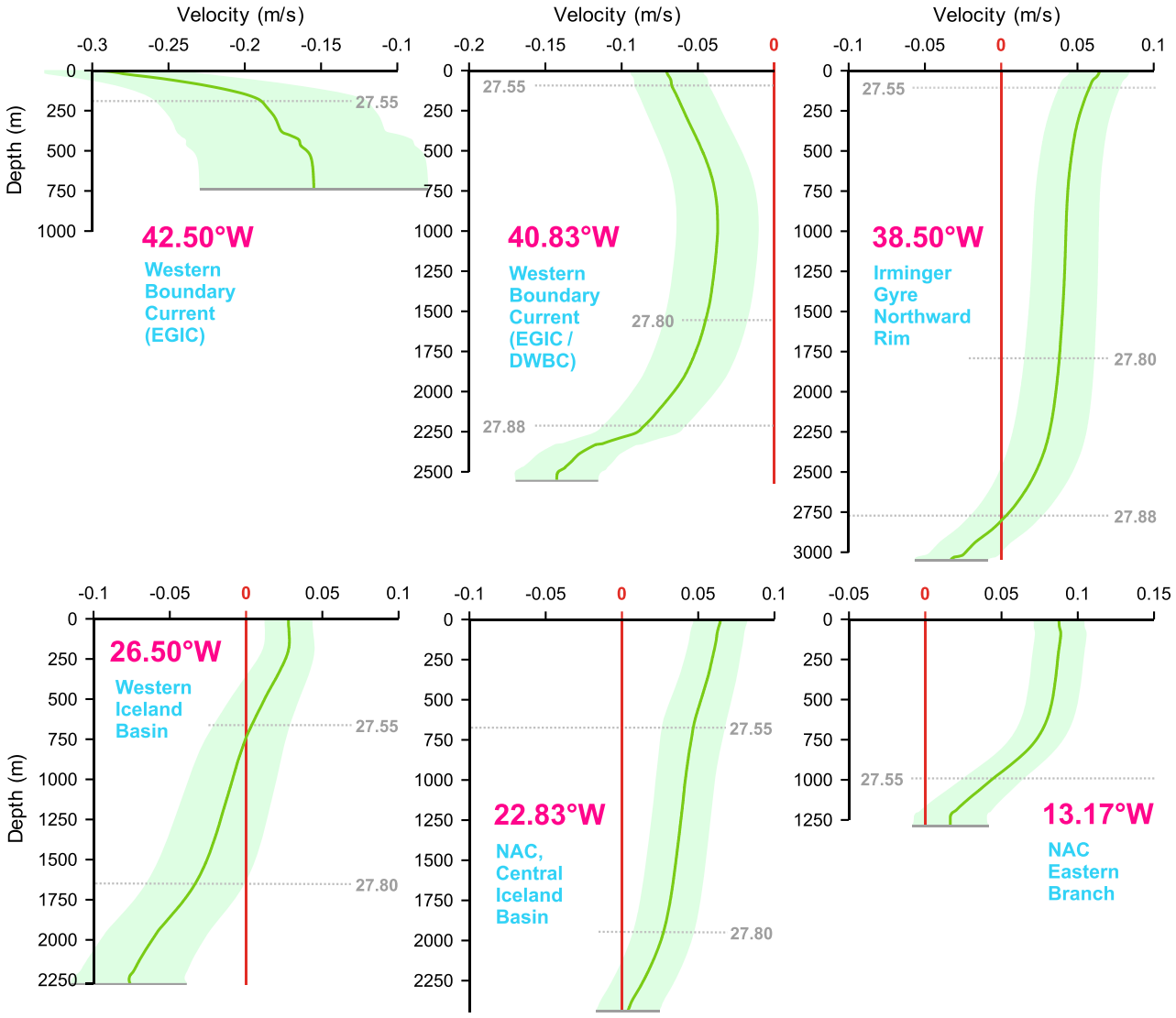

Figure 6. Examples of full-depth vertical profiles of the 2002–2008 mean summer absolute geostrophic velocity (m s^{-1}) across the 59.5°N section. The location (longitude) of each profile is indicated; the profile locations are also marked at the upper axis of Figure 4c. The light green envelopes show the associated uncertainties. Positive velocities are northward. The 2002–2008 mean depths of the σ_0 isopycnals 27.55, 27.80 and, in the Irminger Sea, 27.88 are marked with the gray dotted lines. Abbreviations are explained in the legend to Figure 1.

the v (λ, z) temporal changes and, hence, the uncertainties in the mean v (λ, z) are not statistically independent (e.g., eddies produce vertically and zonally well-correlated v anomalies), the spatial correlation of the v (λ, z) anomalies was to be accounted for. The 7 section repeats do not provide statistically robust information on the spatial structure of the 'baroclinic' variability in the water column. In this situation, the v variability at each longitude was considered coherent in the vertical, and the zonal correlation of the v (λ, z) anomalies was approximated with that of the v (λ, 0) anomalies derived from altimetry.

[28] To test the sensitivity of the derived transports to the definition of the summer season, over which the sea-surface v anomalies are averaged, we excluded the May and/or September altimetry data from the analysis. This had virtually no effect on the results, although such exclusion slightly increased the uncertainties. The test of whether the hydrographic data set adequately defines the mean v structure in the water column was performed by the exclusion of individual section repeats. The transport estimates obtained from six repeat subsets of the hydrographic data (instead of the seven repeats available) differ from those presented in Figure 8 by less than 5%, which is substantially less than the uncertainties in the seven repeat-derived transports.

[29] The most 'rigorous' testing was performed for the western boundary region, where additional hydrographic data are available from the AR7E and Ovide sections [see *Sarafanov et al.*, 2010, Figure 1, Table 1]. The 2008 repeat of the 59.5°N section was excluded from the analysis and the data from the five (2002–2006) of the remaining six repeats were replaced with the AR7E and Ovide data collected in the same years. This substitution led to an increase in the WBC

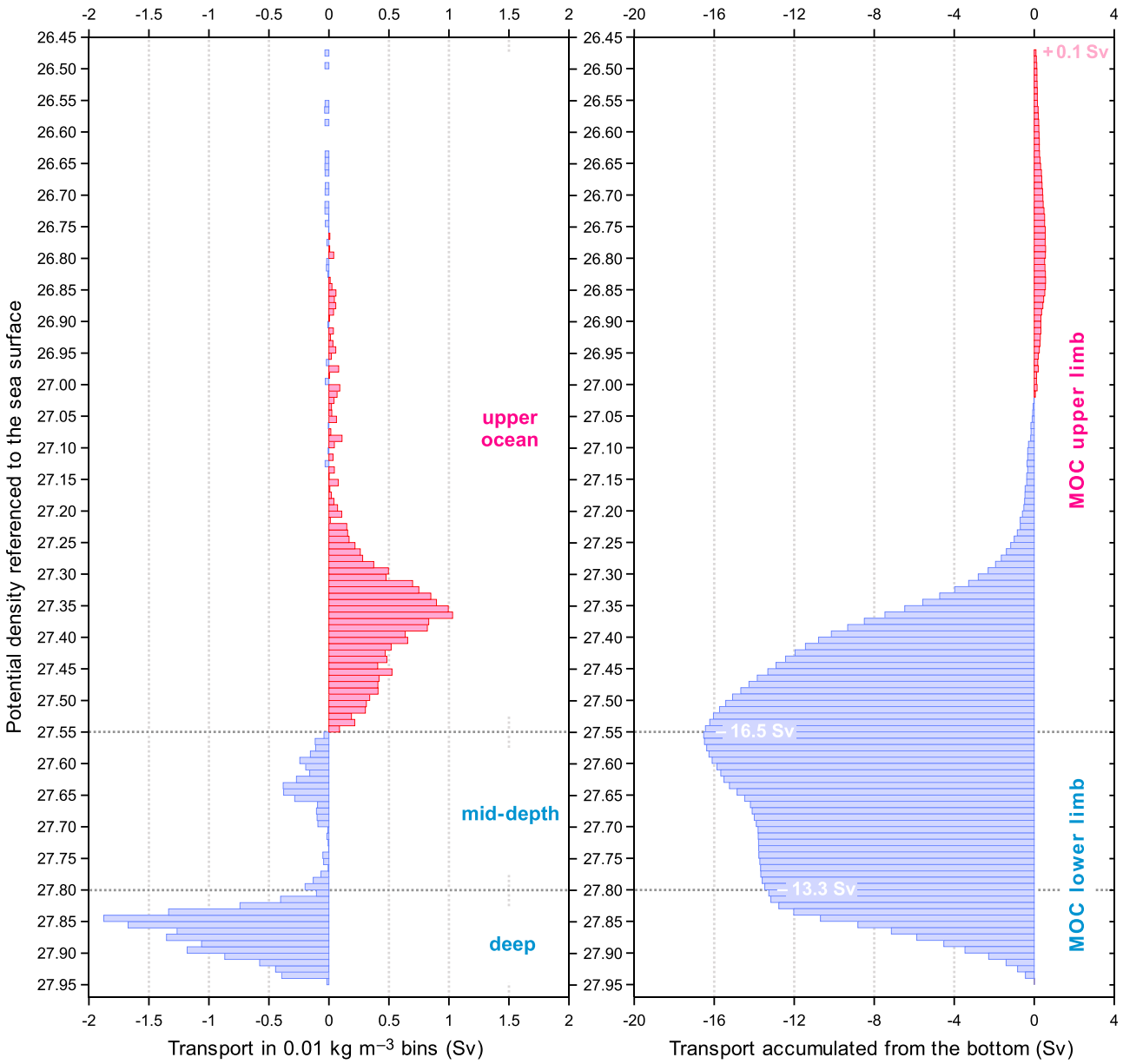

Figure 7. The 2002–2008 mean summer transports (Sv) across 59.5°N as a function of potential density (σ_0). (left) The transports are integrated in 0.01 kg m^{-3} bins and (right) accumulated from the bottom. Positive transports are northward. The horizontal dotted lines indicate the upper boundary of the Nordic overflow-derived deep waters (σ_0 = 27.80) and the density level of extremum in the cumulative transport (σ_0 = 27.55).

transport by about 3%; for instance, the DWBC transport thus obtained appeared only 0.3 Sv larger than the tested value (10.3 ± 1.9 Sv, see Figure 8).

[30] Thus, we made sure that our estimates are barely sensitive to the summer season definition (May–September or, e.g., June–August) and that the mean v structure in the water column is adequately defined from the available hydrographic data. It should be noted that such testing cannot reveal biases in the obtained transports originating from possible biases in the MDT. We address this issue in section 3.4 by comparing the obtained transports with independent estimates.

3.3. Transports Across 59.5°N

[31] The meridional exchange across the 59.5°N section is dominated by the NAC in the eastern basin, the northward Irminger Current (IC) and southward WBC in the Irminger Sea, and the southward deep flow of ISOW in the western Iceland Basin, see Figure 8. The MOCσ intensity is 16.5 ± 2.2 Sv as obtained from a bottom to sea surface accumulation of transports in the density space; the cumulative transport reaches the extremum at σ_0 = 27.55 (Figure 7). A maximum in the overturning stream function quantified in depth coordinates (the MOCz intensity [e.g., *Lherminier et al.*, 2007]) is of 11.2 ± 1.8 Sv at 1180 m depth (no

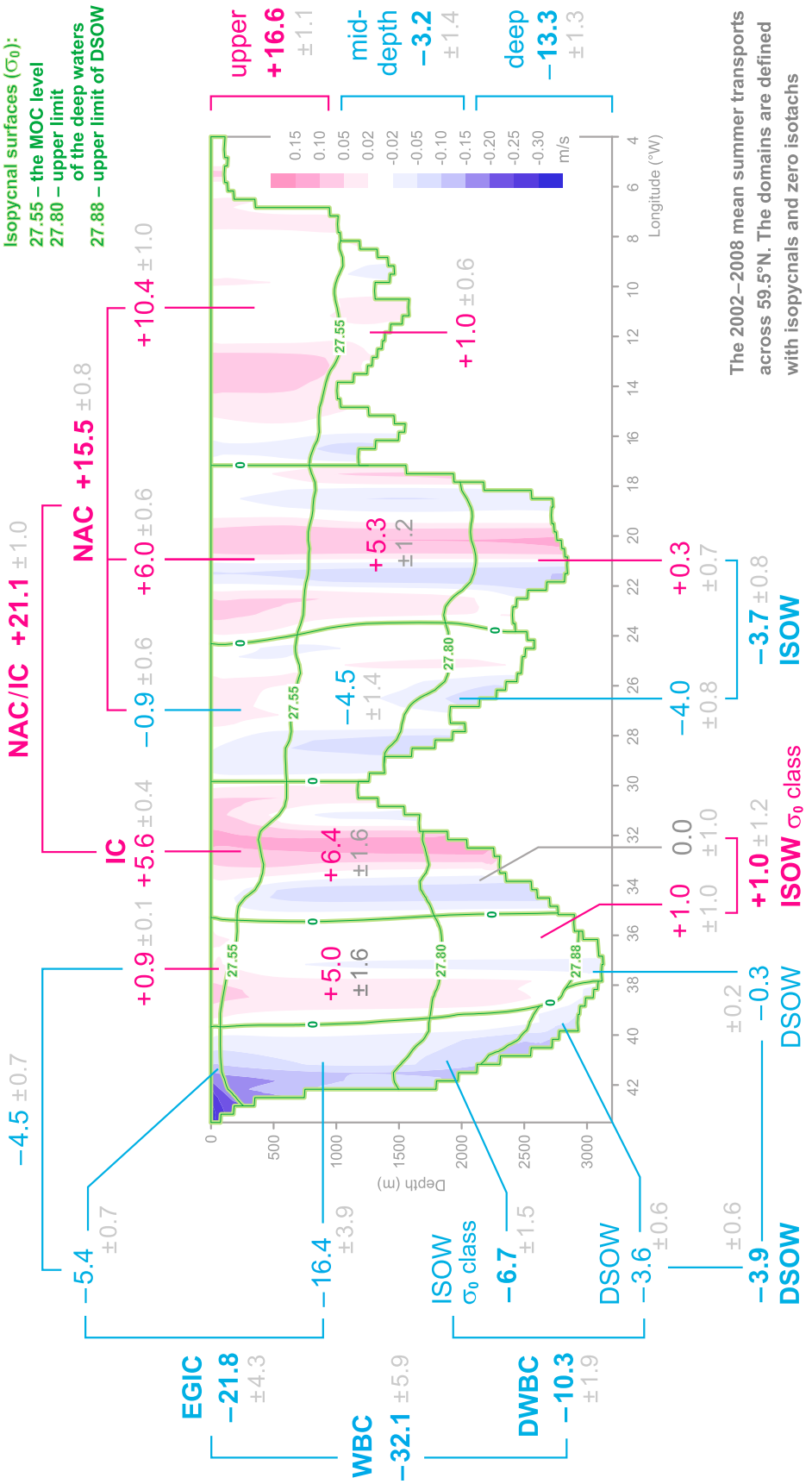

Figure 8. The 2002–2008 mean summer transports (Sv) across 59.5°N. Color shading indicates the mean cross-sectional velocity (v, m s^{-1}), as in Figure 4c. The transports are integrated over the domains (green contours) defined with zero isotachs ($v = 0$) and σ_0 isopycnal surfaces 27.55, 27.80 and, in the Irminger Sea, 27.88. The sign (color) convention is that positive values (in magenta) stand for the northward flows. The uncertainties are shown in gray.

figure shown). The net transport across the section is 0.1 ± 3.0 Sv northward.

3.3.1. Upper Ocean and Middepth Transports

[32] The upper-ocean circulation ($\sigma_0 < 27.55$) shows a distinct cyclonic pattern, the subpolar gyre, composed of almost a section-wide generally northward flow east of ~39°W and a narrow intense southward flow at the western boundary (Figures 4a and 8). The net northward transport in the upper layer (the MOCσ upper limb, 16.6 ± 1.1 Sv) is comprised of the NAC (15.5 ± 0.8 Sv northward, the net upper-ocean transport east of the crest of the Reykjanes Ridge), the IC above the western flank of the Reykjanes Ridge (5.6 ± 0.4 Sv northward), the upper part of the EGIC in the western Irminger Sea (5.4 ± 0.7 Sv southward) and a northward recirculation in the interior Irminger Sea, the Irminger Gyre [*Våge et al.*, 2011] northward rim (0.9 ± 0.1 Sv).

[33] The mid-depth circulation ($27.55 < \sigma_0 < 27.80$) exhibits prominent basin-scale cyclonic patterns in the Irminger Sea and Iceland Basin and a weak net northward flow (1.0 ± 0.6 Sv) east of the Hatton Bank (~17°W). The Iceland Basin cyclonic pattern is composed of the net northward flow in the eastern part of the basin (5.3 ± 1.2 Sv) and the net southward flow above the eastern flank of the Reykjanes Ridge (4.5 ± 1.4 Sv). In the Irminger Sea, the mid-depth southward transport is concentrated in the WBC (16.4 ± 3.9 Sv), and the northward transports occur in the interior and eastern parts of the basin: respectively, in the Irminger Gyre northward rim (5.0 ± 1.6 Sv) and in the IC (6.4 ± 1.6 Sv). Note that the estimate of the IC transport accounts for a southward recirculation (5.1 ± 1.0 Sv) centered at ~34°W.

[34] The net transport in the mid-depth layer is 3.2 ± 1.4 Sv southward. Remarkably, in the LSW density class ($27.70 < \sigma_0 < 27.80$, not shown in Figure 8), the net transport across the section is close to zero (0.5 ± 1.0 Sv southward) implying a minor direct contribution of transports in the LSW density class to the net southward transport in the Atlantic MOCσ lower limb at 59.5°N.

3.3.2. Deep Water Transports

[35] The deep water export to lower latitudes (13.3 ± 1.3 Sv, the net transport of waters denser than $\sigma_0 = 27.80$) is associated primarily with the deep western boundary flows along the East Greenland slope in the Irminger Sea and along the eastern flank of the Reykjanes Ridge in the Iceland Basin (Figure 8).

[36] The southward boundary flow of ISOW in the Iceland Basin (4.0 ± 0.8 Sv) partially recirculates northward (0.3 ± 0.7 Sv, the net flow east of ~24°W), so that the southward export of ISOW from the northern Iceland Basin is 3.7 ± 0.8 Sv.

[37] The DWBC (10.3 ± 1.9 Sv) in the Irminger Sea carries 6.7 ± 1.5 Sv and 3.6 ± 0.6 Sv in the ISOW ($27.80 < \sigma_0 < 27.88$) and DSOW ($\sigma_0 > 27.88$) density classes, respectively. In the Irminger Sea interior, between ~35°W and the zero isotach enclosing the DWBC, the net transport is northward in the ISOW density class (1.0 ± 1.0 Sv, 35–39°W), being concentrated primarily in the Irminger Gyre northward rim (~38–39°W), and southward in the DSOW layer (0.3 ± 0.2 Sv, 36–38°W). Accordingly, the total southward transport in the DSOW layer is estimated at 3.9 ± 0.6 Sv: ~3.6 Sv in the DWBC and ~0.3 Sv in the interior part of the basin.

[38] In the eastern Irminger Sea, 3.8 ± 0.7 Sv of waters denser than $\sigma_0 = 27.80$ is transported northward along the western flank of the Reykjanes Ridge in the deep extension of the IC (32–33°W). This flow carries ISOW arriving to the Northwest Atlantic from the Iceland Basin through the Charlie-Gibbs Fracture Zone (CGFZ, Figure 1) [e.g., *Schmitz and McCartney*, 1993; *Saunders*, 1994] and, likely, from other deep passages in the Reykjanes Ridge north of the CGFZ [e.g., *Xu et al.*, 2010]. The eastern boundary pathway of ISOW into the Irminger Sea is a common feature of all regional circulation schemes [e.g., *Schmitz and McCartney*, 1993; *Schott and Brandt*, 2007; *Lherminier et al.*, 2010; *Xu et al.*, 2010], which also suggest that the fate of the ISOW northward flow is to recirculate southwestward and join the DWBC in the Irminger Sea (Figure 1).

[39] The notion that the DWBC is the major conduit for the ISOW outflow from the Irminger Sea has recently been called into question by *Sarafanov et al.* [2007], who noticed the absence of distinct hydrographic (salinity, oxygen and silicate) signatures of ISOW in the vicinity of the East Greenland slope and hypothesized the existence of an interior pathway of ISOW from the Irminger Sea. The present analysis reveals such pathway at ~33–35°W in the deep extension of the IC southward recirculation that carries essentially the same amount of ISOW (3.8 ± 0.8 Sv) with nearly the same properties (see Figure 9) as the deep extension of the IC carries northward. It should be noted that the presence of the IC subsurface recirculation in the 2000s also follows from the analysis by *Våge et al.* [2011, Figure 10d]; this feature was not, however, discussed by *Våge et al.* [2011], as the main focus of that study was on the Irminger Gyre and boundary flows.

[40] After crossing 59.5°N, a part of the ISOW southward recirculation might retroflect back into the interior Irminger Sea (at ~35–39°W, where the deep water transport is generally northward) and eventually contribute to the DWBC. This would explain low oxygen concentrations and increased salinity in the ISOW density class at 35–39°W, as well as at the eastern periphery of the DWBC at ~39–40°W (see Figure 9). A maximum contribution of the ISOW flow to the DWBC at 59.5°N can be estimated from the net northward transport in the ISOW density class in between the DWBC and the western slope of the Reykjanes Ridge. The latter net northward transport (1.0 ± 1.2 Sv) makes ~15% of the DWBC transport in the ISOW density class and ~10% of the total DWBC transport. Apparently, a part of the net northward flow east of the DWBC is associated with the DWBC recirculation, and hence the ISOW contribution to the DWBC in the 2000s could be even less than ~10%.

[41] The 2002–2008 mean distributions of salinity (S) and oxygen concentrations (O_2) at 59.5°N imply that the ISOW fraction in the DWBC is indeed minor. We demonstrate this in Figure 9. It is evident in the S-O_2 space (Figure 9c) that waters transported by the DWBC in the ISOW density class have nearly the same properties (layer-averaged S and O_2) as if they were a product of upstream diapycnal mixing of waters transported by the WBC in the layers above ($27.76 < \sigma_0 < 27.80$, 'deep LSW') and below ($\sigma_0 > 27.88$, DSOW) the ISOW density class. Indeed, the S-O_2 index for the ISOW density class in the DWBC is very close to the 'deep LSW'–DSOW mixing line, though deviates from the latter toward higher salinity. As follows from solving the 'deep

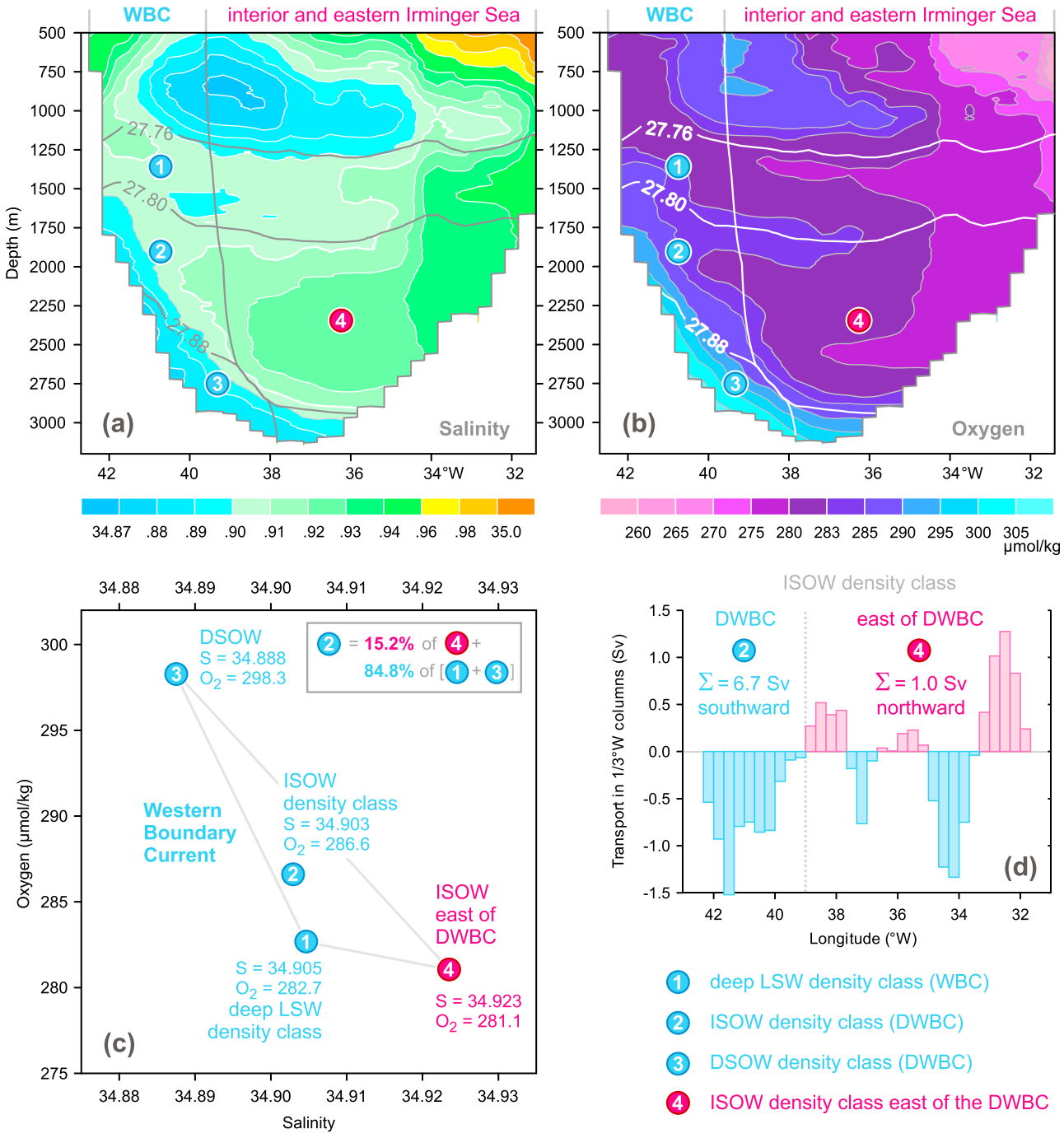

Figure 9. On the composition of waters transported by the DWBC in the ISOW density class in the Irminger Sea at 59.5°N. The 2002–2008 mean (a) salinity (S) and (b) oxygen (O_2, μmol kg^{-1}) distributions at 59.5°N are overlaid with a zero isotach enclosing the Western Boundary Current (WBC) and the σ_0 isopycnals 27.76, 27.80 and 27.88. The numbers in the circles refer to the following four domains: the (1) deep LSW ($27.76 < \sigma_0 < 27.80$), (2) ISOW ($27.80 < \sigma_0 < 27.88$) and (3) DSOW ($\sigma_0 > 27.88$) density classes in the WBC, and (4) the ISOW density class ($27.80 < \sigma_0 < 27.88$) off the DWBC. (c) The S-O_2 diagram for the domain-averaged properties; the diagram implies a minor fraction (~15%) of the ISOW observed off the DWBC (domain 4) in waters transported by the DWBC in the ISOW density class (domain 2). (d) Zonal distribution of the 2002–2008 mean transports (Sv) across 59.5°N in the ISOW density class. The transports are integrated in 1/3° longitudinal bins and plotted as a function of longitude. Positive transports are northward. The vertical dotted line indicates the DWBC eastern limit (39°W).

LSW'–DSOW–ISOW mixing triangle, a fraction of only ~15% of the off-DWBC ISOW (32–39°W) in the three-component mixture is enough to explain that deviation. Although the estimate is tentative, as it relies upon a simplified view of mixing within and off the WBC, it indicates that the transport pattern-based inference about a minor contribution of ISOW to the DWBC at 59.5°N does not contradict the tracer distributions. The net southward export of deep waters from the Irminger Sea is 9.6 ± 1.2 Sv.

3.4. Comparison With Independent Transport Estimates

[42] The present estimate of the mean transports across the 59.5°N section employs, inter alia (see section 3.1), the mean sea-surface velocities derived from the Rio05 MDT. In a number of recent studies [e.g., *Gourcuff*, 2008; *Våge et al.*, 2011; *Gourcuff et al.*, 2011], the Rio05 MDT product has been used, along with altimetry, to reference the hydrography-derived velocity profiles, and a generally good agreement between thus estimated transports and those obtained from direct velocity measurements has been reported.

[43] The MDT and altimetry are known to be less accurate at the ocean boundaries. *Våge et al.* [2011] noticed that their estimate of the 1991–2007 mean WBC transport (39 ± 4 Sv at the AR7E line, 59.5–60°N) "is in the upper range of the previous transport estimates" and cautiously attributed the discrepancy to a likely local bias in the AVISO absolute velocities built upon the Rio05 MDT. The results by *Gourcuff et al.* [2011, Table 4, Figure 9] obtained practically for the same location (~58–60°N, A25 and Ovide sections), but using a somewhat different processing of the Rio05 MDT, on the contrary, imply an underestimation of the EGIC (WBC, $\sigma_0 < 27.80$) transport by 1–4 Sv. For the NAC transport, no systematic bias has been found [*Gourcuff et al.*, 2011, Table 4, Figure 9]. The apparent contradiction between the results by *Våge et al.* [2011] and *Gourcuff et al.* [2011] with respect to the sign of a bias in the WBC transport highlights the complexity of assessing the boundary circulation by combining hydrography with MDT and altimetry, as well as the fact that thus obtained transports require verification.

[44] The available MDT-independent estimates of the WBC transport at Cape Farewell and of the MOCσ intensity at Cape Farewell to European coast sections are plotted in Figure 10 along with the 2002–2008 mean transports obtained in the present study. For the WBC, the comparison is performed for the sea surface-to-bottom transport of the current and, in order to verify whether the vertical structure of the WBC transport is adequately reproduced in our analysis, for the transports by the upper (EGIC, $\sigma_0 < 27.80$) and lower (DWBC, $\sigma_0 > 27.80$) parts of the WBC.

[45] The comparison is quite favorable. Our results differ from the averages of the independent estimates by less than 1 Sv, which is less than the uncertainties in the averaged independent transports. Our estimate of the top-to-bottom WBC transport (32.1 ± 5.9 Sv) is in a close agreement with the independent estimates averaged both over the entire set (32.0 ± 2.7 Sv, 1978–2006) and over the 2000s (32.1 ± 4.8 Sv, 2002–2006). The same is true for the EGIC and DWBC transports.

[46] For the MOCσ, only five estimates (1992–2006) are available to compare with. These estimates range from 11.4 ± 2.4 Sv to 18.5 ± 2.4 Sv, and the mean of the five estimates, 15.9 ± 1.9 Sv, is highly sensitive to the exclusion of the extreme values. Two of the three estimates of the MOCσ obtained in the 2000s from the Ovide data, 16.2 ± 2.4 Sv in 2002 and 16.4 ± 2.4 Sv in 2004, are very close to our estimate of 16.5 ± 2.2 Sv. In line with our analysis, the 'interface' between the MOCσ upper and lower limbs has been found at Ovide around the σ_1 = 32.1 isopycnal [*Lherminier et al.*, 2007, 2010], which practically coincides with σ_0 = 27.55.

[47] By combining mooring data collected at 59.5–60°N in the Irminger Sea in 2004–2006 with altimetry-derived velocity anomalies, *Daniault et al.* [2011b] reconstructed the (MDT-independent) 1992–2009 time series of the WBC transport between the 200 m and 2000 m isobaths. When integrated within the same limits, the WBC transport obtained herein differs by only 0.2 Sv from the 2002–2008 mean summer transport from the time series by *Daniault et al.* [2011b].

[48] Another important quantity to be checked is the net mean transport across 59.5°N. The net transport across transatlantic sections is usually inferred as the algebraic sum of volume fluxes into and from the Arctic Ocean (Davis and Bering straits throughflows, net precipitation and river discharge) and used in transport estimates as the main constraint on the inverse model solutions. For the sections between Greenland and Europe, this constraint is typically set at zero or 1 Sv northward [see *Bacon*, 1997; *Lumpkin and Speer*, 2007; *Lherminier et al.*, 2007, 2010]. In our estimate, no constraints are applied, and a nearly zero net transport (0.1 ± 3.0 Sv northward) results from the integration of transports over the whole section.

[49] Finally, our estimate of the ISOW southward export from the northern Iceland Basin, 3.7 ± 0.8 Sv, can be compared with the measured overflow/ISOW transports across the Iceland-Scotland Ridge and in the northern Iceland Basin. The comparison is again favorable. The mean overflow transport from the Norwegian Sea into the Iceland Basin is about 3.1 Sv, as obtained from long-term mooring measurements in the 1990s–2000s [*Hansen and Østerhus*, 2007; *Olsen et al.*, 2008]. Downstream, at the head of the Iceland Basin at ~62–63°N, the mean overflow/ISOW transport of 3.2 ± 0.5 Sv ($\sigma_0 > 27.80$) was estimated by *Saunders* [1996] from nearly 1-yearlong mooring record. Because of entrainment, the ISOW transport is expected to show an increase along the ISOW pathway from the northern Iceland Basin to 59.5°N. So, the net ISOW transport of ~3.7 Sv resulting from our analysis seems to be consistent with the upstream observations. The comparison is tentative, though, because the mooring measurements at 62–63°N were made in 1990–1991 [*Saunders*, 1996] and because of the unknown entrainment rate in between the Iceland-Scotland Ridge and 59.5°N. On the other hand, the recently reported stability of the overflow transport on a decadal time scale [*Olsen et al.*, 2008] implies that our estimate of the mean ISOW transport and the estimate by *Saunders* [1996] are still comparable.

[50] To summarize, the mean transports obtained in the present study show a remarkable consistency with MDT-independent estimates, where the latter are available. The caveat is that the synoptic estimates, we largely rely upon (Figure 10), are scarce and widely scattered, and therefore

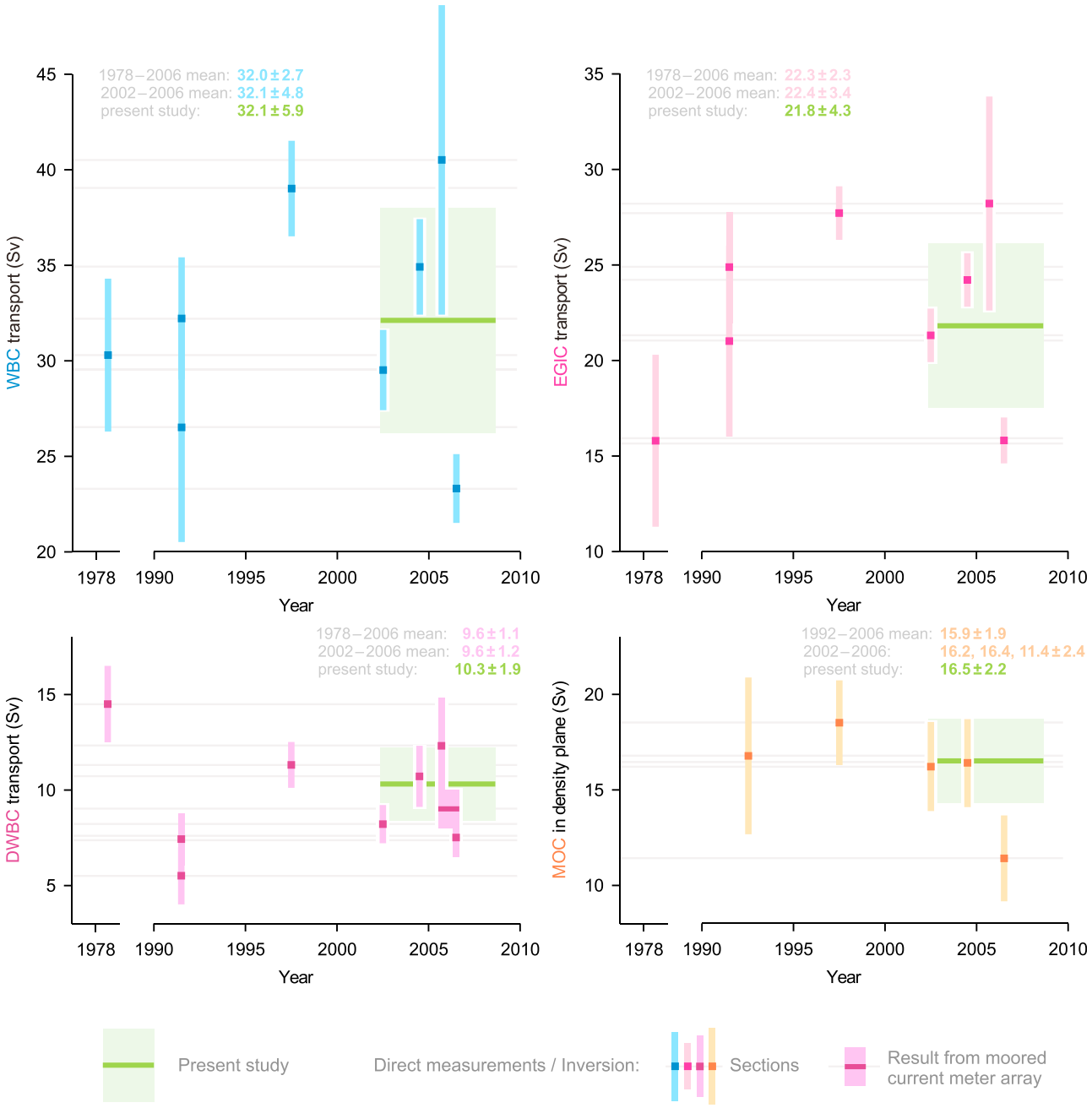

Figure 10. Comparison of the mean transports (Sv) obtained in the present study with independent transport estimates as available for the top to bottom WBC, EGIC (the WBC upper part, $\sigma_0 < 27.80$), DWBC (the WBC lower part, $\sigma_0 > 27.80$) and the MOCσ. The light bars show the uncertainties. The independent estimates, except the April 1978 WBC transport [see *Clarke*, 1984; *Bacon and Saunders*, 2010] and the September 2005 to June 2006 mooring record-derived DWBC transport [*Bacon and Saunders*, 2010], are based on shipboard hydrographic/velocity measurements made in summer months (June–September) in 1991 [*Bersch*, 1995; *Bacon*, 1997], 1992 [*Lumpkin and Speer*, 2007], 1997 [*Lherminier et al.*, 2007], 2002, 2004 [*Lherminier et al.*, 2010], 2005 [*Holliday et al.*, 2009] and 2006 [*Gourcuff et al.*, 2011]. The MOCσ estimates are from the AR7E (1992) [*Lumpkin and Speer*, 2007], A25 (1997) and Ovide (2002–2006) [*Lherminier et al.*, 2007, 2010; *Gourcuff*, 2008] Cape Farewell to European coast sections.

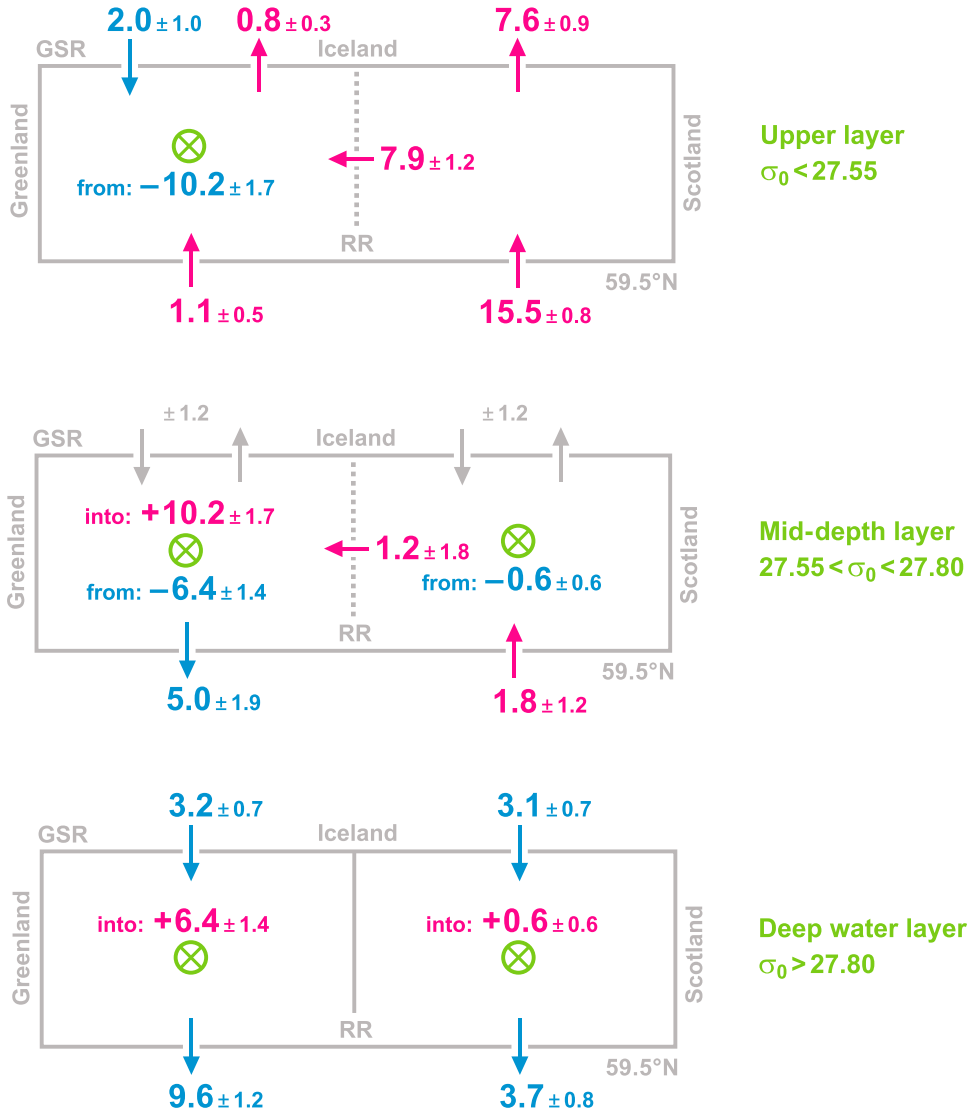

Figure 11. A three-layer box model of the large-scale circulation in the North Atlantic in between the 59.5°N section and the Greenland-Scotland Ridge (GSR). The transports (Sv) at the southern boundary are the mean transports across 59.5°N as obtained in the present study. The transports at the northern boundary (GSR) are defined as explained in section 4. The boundary between the western and eastern boxes (the Reykjanes Ridge (RR)) is closed (open) for the deep (upper-ocean and mid-depth) circulation. The diapycnal volume fluxes (crossed green circles, transports into the layers are positive) and transports across the RR are inferred from the condition of volume conservation in each box/layer. The uncertainties in the inferred 'output' transports are defined as the square root of the sum of the squared uncertainties in the 'input' transports across 59.5°N and the GSR. The estimated uncertainty in the 0.6 Sv flux into the deep layer east of the RR, ± 1.1 Sv, was reduced to ± 0.6 Sv based on a priori knowledge that ISOW does entrain warmer Atlantic waters and hence the flux is 'downward'. The northward (southward) and westward transports are shown in magenta (cyan), as well as the diapycnal fluxes into (from) the layers.

the averages of these estimates should be regarded as tentative reference values only.

4. Interbasin and Diapycnal Transports in the Atlantic Ocean North of 59.5°N

[51] Quantitative estimates of the main components of the North Atlantic–Nordic Seas exchange across the Greenland-Scotland Ridge (GSR) are available owing to the long-term monitoring programs [*Macrander et al.*, 2005; *Østerhus et al.*, 2005, 2008; *Dickson et al.*, 2008] and synoptic measurements [*Sutherland and Pickart*, 2008]. We use these estimates along with the present estimate of the mean transports across 59.5°N to infer the mean integral transport across the Reykjanes Ridge and diapycnal volume fluxes in between the 59.5°N section and the GSR.

[52] A simple box model is applied, see Figure 11. Following the approach by *Lherminier et al.* [2010], we subdivided the 59.5°N–GSR region into two domains: to the west and to the east of the Reykjanes Ridge; the western

domain thus corresponds to the Irminger Sea. In the vertical, the water column is split into the three layers, for which the integral transports across 59.5°N are assessed: the upper (σ_0 < 27.55, the MOCσ upper limb), mid-depth (27.55 < σ_0 < 27.80) and deep water (σ_0 > 27.80) layers.

[53] At the southern border (59.5°N), the transports into/from the boxes are the mean transports across the 59.5°N section (see Figure 8). At the northern border (GSR), the transports are imposed as follows. The exchange between the Greenland and Irminger seas (western box) is attributed to the Iceland branch of the Atlantic Inflow (0.8 ± 0.3 Sv northward) and the East Greenland Current (2.0 ± 1 Sv southward) in the upper layer, and the Denmark Strait Overflow (3.2 ± 0.7 Sv southward) in the deep layer [see *Østerhus et al.*, 2005; *Sutherland and Pickart*, 2008; *Macrander et al.*, 2005]. The Northeast Atlantic–Norwegian Sea exchange (eastern box) is attributed to the Faroe and Shetland branches of the Atlantic Inflow (7.6 ± 0.9 Sv northward) in the upper layer and the Iceland Scotland Overflow into the Iceland Basin (3.1 ± 0.7 Sv southward) in the deep layer [*Østerhus et al.*, 2005, 2008; *Olsen et al.*, 2008]. The resulting net transport across the GSR (0.1 Sv northward) is the same as that across 59.5°N; the MOCσ intensity defined by the total overflow transport is 6.3 ± 1 Sv.

[54] In the above solution, the unknown net transports in the mid-depth layer on both sides of Iceland are assumed negligible compared to the upper-ocean and overflow transports across the GSR and the mid-depth transports across 59.5°N. The uncertainty associated with the net mid-depth exchange across the GSR is imposed equal to the uncertainty in the sum of the upper-ocean and overflow transports (±1.7 Sv) and shared equally between the western and eastern boxes (±1.2 Sv in each box). In the absence of sustained measurements of the East Greenland Current transport in the Denmark Strait, we inevitably rely upon the synoptic estimate by *Sutherland and Pickart* [2008] and put a ± 50% uncertainty on it. We assume that the combination of the 2002–2008 mean transports across 59.5°N with the available estimates of the Atlantic Inflow and overflow transports is appropriate despite the fact that the latter estimates are based mostly on the data from the late 1990s to the early to mid-2000s. The stability of the Atlantic–Nordic Seas exchange on a decadal time scale [*Olsen et al.*, 2008; *Hansen et al.*, 2010; *Mork and Skagseth*, 2010] brings confidence that this assumption is suitable. Seasonal signals in the transports across the GSR are neglected, since they are small compared to the uncertainties in the mean transports and not evidenced for all exchange components [see *Macrander et al.*, 2005; *Østerhus et al.*, 2005, 2008; *Hansen et al.*, 2010].

[55] After the input transports were defined, the sought volume fluxes between the basins and layers were calculated from the condition of volume conservation in each box/layer. The upper-ocean (7.9 ± 1.2 Sv) and mid-depth (1.2 ± 1.8 Sv) transports across the Reykjanes Ridge are westward, and the inter-layer diapycnal fluxes are 'downward' (Figure 11). This reflects the essential nature of the large-scale circulation in the northern North Atlantic: a part of waters transported by the NAC and IC recirculates cyclonically in the subpolar gyre, gains density due to cooling and overturns feeding the return lower limb of the MOC.

[56] The total diapycnal volume flux across the σ_0 = 27.55 isopycnal in the 59.5°N–GSR region is estimated at 10.2 ± 1.7 Sv. This flux associated with light-to-dense conversion (overturning) of the upper-ocean waters, allies with the total overflow transport of ~6 Sv to compose the net southward export of 16.5 ± 2.2 Sv in the MOCσ lower limb at 59.5°N. There are strong reasons to suggest that the ~10 Sv flux across σ_0 = 27.55 occurs, apparently in winter, in the Irminger Sea rather than to the east of the Reykjanes Ridge. In summer at 59.5°N, the zonal-mean depth of the σ_0 = 27.55 isopycnal in the interior and western Irminger Sea is ~140 m, which is substantially less than the mean winter mixed layer depth of 300–400 m in the 2000s [see *Våge et al.*, 2009, Figure 2]. Accordingly, in the Irminger Sea, wintertime convective mixing certainly overturns the upper-ocean waters into the mid-depth layer (27.55 < σ_0 < 27.80). East of the Reykjanes Ridge in summer, the σ_0 < 27.55 layer is much thicker: its thickness increases in the eastward direction from ~600 m to ~1000 m, and the σ_0 = 27.55 isopycnal corresponds there to a persistent oxygen minimum (Figure 5c) [see also *Sarafanov et al.*, 2008, Figure 2]. Thus, the mid-depth layer (27.55 < σ_0 < 27.80) east of the Reykjanes Ridge is unlikely to be considerably affected by wintertime ventilation, at least immediately north of 59.5°N.

[57] The suggestion that the upper-ocean waters enter the σ_0 > 27.55 layer in the Irminger Sea is supported by sea surface density data collected in the northern North Atlantic. *McCartney and Talley* [1982] documented the gradual along-path density gain by the upper-ocean waters carried by the NAC/IC and discussed this process in the context of the Subpolar Mode Water transformation in the subpolar gyre. The winter mixed layer densities of σ_0 > 27.55 were observed west of the crest of the Reykjanes Ridge in the Irminger and Labrador seas [*McCartney and Talley*, 1982, Figure 6a]. Climatology of the winter sea surface density [*Thierry et al.*, 2008, Figure 9] shows that north of 59.5°N the mean February outcropping of the σ_0 = 27.55 isopycnal is practically collocated with the crests of the Reykjanes Ridge and the Iceland-Scotland Ridge. Accordingly, north of 59.5°N in winter, the upper-ocean waters are denser than σ_0 = 27.55 in the Irminger Sea and lighter than σ_0 = 27.55 east of the Reykjanes Ridge. In the context of the overturning in the density space, this means that the densification of the NAC/IC-derived waters culminates in the Irminger Sea, where these waters eventually gain density of σ_0 > 27.55 and thereby enter the MOCσ lower limb. Remarkably, no deep convection is needed for this (~10 Sv) overturning.

[58] The total volume flux across σ_0 = 27.80 in the 59.5°N–GSR region is estimated at 7.0 ± 1.5 Sv. The volume flux into the deep layer in the Iceland Basin (~0.6 Sv) can be interpreted as the net entrainment by ISOW along its pathway from the Iceland-Scotland sills to the 59.5°N section. The diapycnal flux across σ_0 = 27.80 in the Irminger Sea, 6.4 ± 1.4 Sv, is nearly 10 times larger than that in the Iceland Basin. Accordingly, nearly half of the ~13 Sv net southward flow of deep waters across 59.5°N in the 2000s was fed by the Nordic Seas overflows, and another half was due to entrainment of the Atlantic waters that occurred predominantly in the Irminger Sea.

5. Synthesis of the Results and Conclusion

[59] By combining the 2002–2008 repeat hydrography at 59.5°N, MDT, altimetry and observation-based estimates of

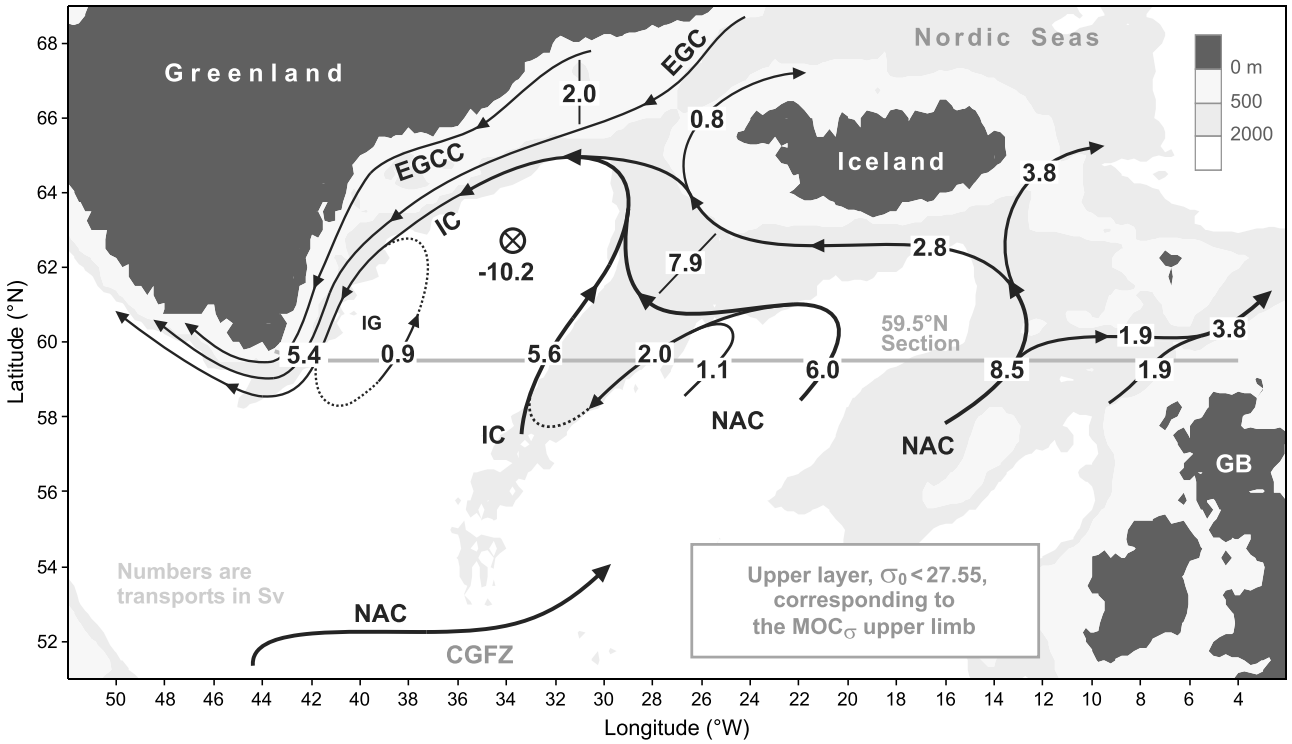

Figure 12. Schematic diagram of the large-scale circulation and transports (Sv) in the upper layer ($\sigma_0 >$ 27.55), corresponding to the MOCσ upper limb. The uncertainties in the transport estimates are shown in Figures 8 and 11. The crossed circle denotes the diapycnal volume flux across $\sigma_0 = 27.55$, i.e., the 'downward' flux from the layer. The dotted curves indicate the assumed pathways. IG, Irminger Gyre [see *Våge et al.*, 2011]. Other abbreviations are explained in the legend to Figure 1.

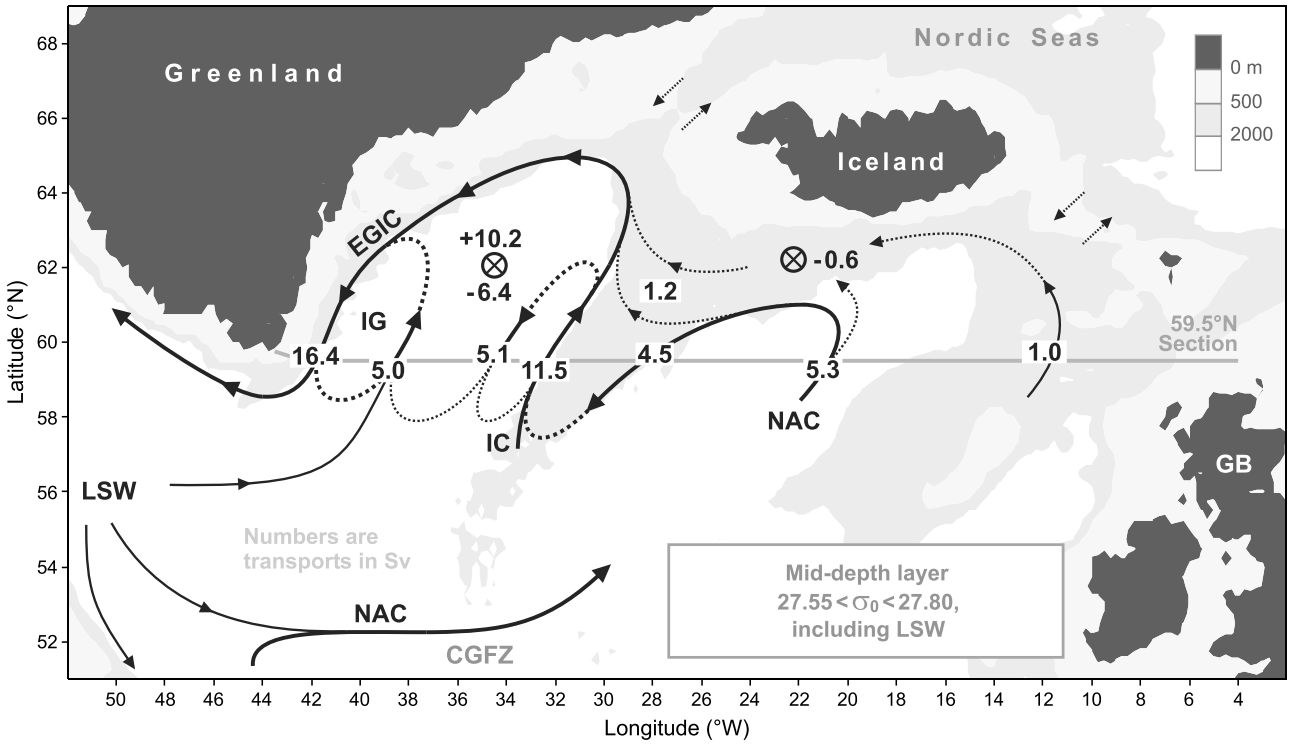

Figure 13. As in Figure 12 but for the mid-depth layer ($27.55 < \sigma_0 <$ 27.80), including the Labrador Sea Water (LSW) density class ($27.70 < \sigma_0 >$ 27.80). The diapycnal volume fluxes into (from) the layer are positive (negative).

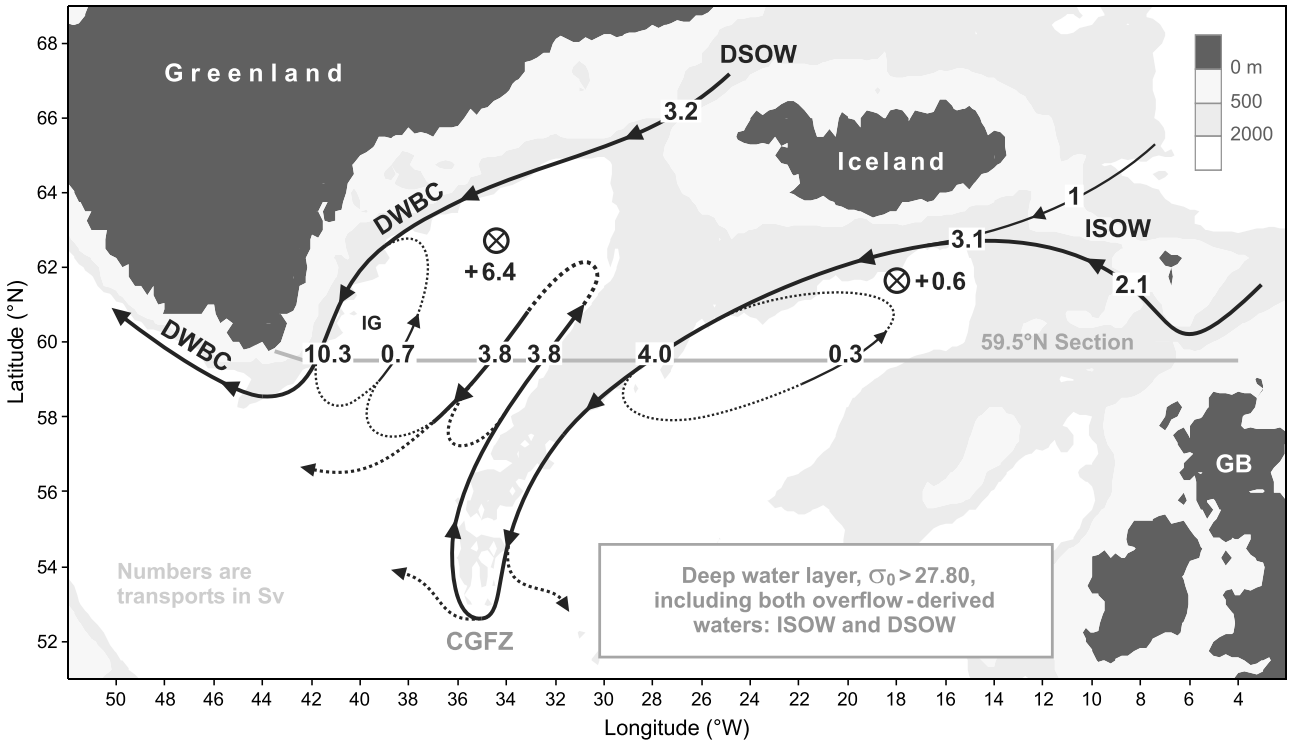

Figure 14. As in Figure 13 but for the deep water layer ($\sigma_0 > 27.80$), including the Denmark Strait and Iceland-Scotland overflow-derived waters.

the Atlantic–Nordic Seas exchange, we assessed a mean state of the full-depth summer circulation in the North Atlantic in between Cape Farewell (Greenland), Scotland and the Greenland-Scotland Ridge (GSR).

[60] The upper-ocean, mid-depth and deep water circulation patterns, merging the results of the present analysis with those from the earlier studies [e.g., *Macrander et al.*, 2005; *Østerhus et al.*, 2005, 2008; *Schott and Brandt*, 2007; *Sutherland and Pickart*, 2008; *Lherminier et al.*, 2010; *Våge et al.*, 2011], are schematically visualized in Figures 12–14. A schematic diagram of the meridional overturning circulation in the Atlantic Ocean north of 59.5°N is displayed in Figure 15.

[61] The results provide a conceptual view of the gyre/overturning circulation at the northern periphery of the Atlantic Ocean in the 2000s.

[62] The NAC and IC collectively carry 21.1 ± 1.0 Sv of warm upper-ocean waters across 59.5°N northward within the MOCσ upper limb ($\sigma_0 < 27.55$). About 40% of this flow forms the Atlantic Inflow to the Nordic Seas, and 60% (12.7 ± 1.4 Sv) recirculates westward in the subpolar gyre northern limb south of Iceland to feed the WBC in the Irminger Sea. The recirculating NAC/IC-derived waters cool and gain density, and only 20% (2.5 ± 1.2 Sv) of these waters exits the Irminger Sea in the WBC at shallow levels ($\sigma_0 < 27.55$), while 80% (10.2 ± 1.7 Sv, a half of the NAC/IC northward flow across 59.5°N) enters the MOCσ lower limb ($\sigma_0 > 27.55$). The resulting net southward transport in the MOCσ lower limb at the latitude of Cape Farewell is 16.5 ± 2.2 Sv, of which ∼60% (∼10.2 Sv) is due to light-to-dense water conversion south of the GSR.

[63] As no dense-to-light water conversion is expected to occur in the subpolar gyre, the NAC/IC-derived waters, once entering the MOCσ lower limb in the Irminger Sea, will eventually contribute to the MOCz lower limb (∼11 Sv at 59.5°N) at the southern margin of the subpolar region. There, at ∼48°N, the MOCσ and MOCz are of nearly the same magnitude, 16 ± 2 Sv, as estimated from data collected in the 1990s [see *Schott and Brandt*, 2007; *Lumpkin et al.*, 2008]. This is very close to our estimate of the mean MOCσ at 59.5°N. The comparison is tentative, though, because it does not take into account the decadal variability of the MOC [*Koltermann et al.*, 1999; *Willis*, 2010]. With this caveat in mind, our results imply a minor effect on the MOCσ magnitude by the net dense water production in the subpolar gyre in between ∼48°N and 59.5°N. This inference concurs with the results by *Pickart and Spall* [2007] suggesting a minor contribution to the magnitude of the North Atlantic MOC by the net water mass transformation in the Labrador Sea.

[64] To conclude, the results of the present study, verified with independent estimates where possible, provide the first observation-based quantitative view of a mean state of the gyre/overturning circulation at the northern periphery of the Atlantic Ocean. The most interesting features of the obtained circulation pattern are as follows:

[65] 1. Nearly half of volume of the upper-ocean waters transported northward across 59.5°N in the eastern limb of the subpolar gyre (NAC and IC, $\sigma_0 < 27.55$) overturns in the density plane in between 59.5°N and the GSR and feeds the lower limb of the Atlantic MOCσ.

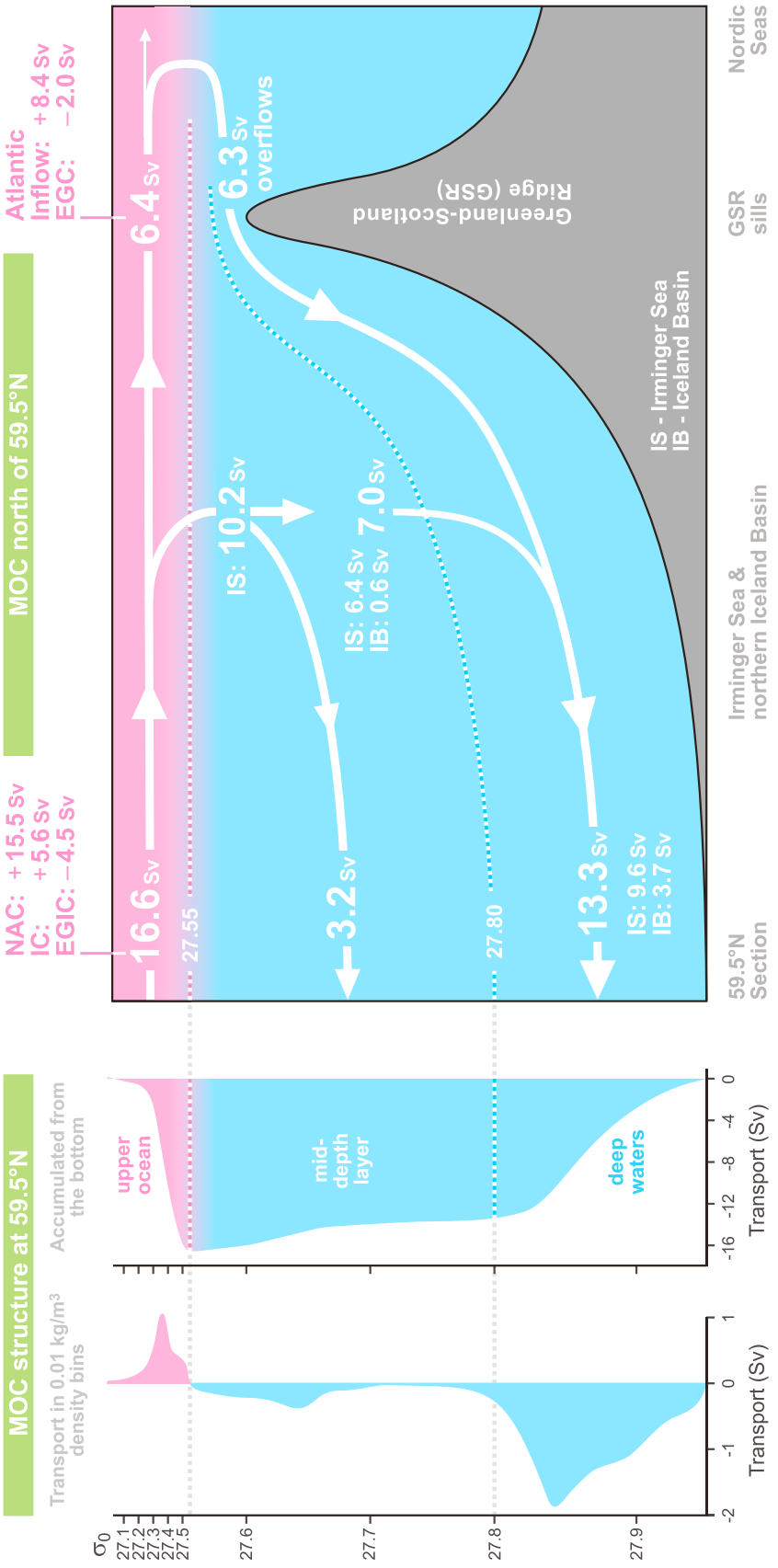

Figure 15. Schematic diagram of the Meridional Overturning Circulation (MOC) at the northern periphery of the Atlantic Ocean, northeast of Cape Farewell. The MOC vertical structure at 59.5°N, shown on the left, represents a generalized version of Figure 7; note the different scales of the ordinate axes above and below $\sigma_0 = 27.55$. The dotted lines refer to the σ_0 isopycnals 27.55 and 27.80. The arrows in the right plot denote the integral meridional and diapycnal volume fluxes; the associated uncertainties are shown in Figures 8 and 11. Where the signs are specified, the positive (negative) transports are northward (southward). The NAC and EGIC transports in the upper layer ($\sigma_0 < 27.55$) at 59.5°N are the throughputs accounting for the recirculations (see Figures 8 and 12). IS and IB stand for the Irminger Sea and Iceland Basin, respectively.

[66] 2. The contribution to the MOCσ lower limb at 59.5°N by overturning (light-to-dense water conversion) of the NAC/IC-derived upper-ocean waters south of the GSR is one and a half times larger than the contribution of the Nordic Seas overflows.

[67] 3. The net southward flow in MOCσ lower limb at 59.5°N is associated primarily with the deep water (σ_0 > 27.80) export. Nearly half of the net southward flow of deep waters across 59.5°N is due to entrainment of the Atlantic waters in the Irminger Sea.

[68] 4. The DWBC at 59.5°N is fed primarily by the Denmark Strait Overflow and by the diapycnal flux/entrainment from the mid-depth layer, while the contribution to the DWBC transport from the ISOW flow is minor. A major part of the ISOW transported into the Irminger Sea in the deep extension of the Irminger Current recirculates southward in the eastern Irminger Sea and exits the basin via an interior pathway rather than along the western boundary.

[69] The results can be used for validation of numerical models. From this perspective, multiyear mean transports have an obvious advantage over individual section-based synoptic estimates, which bear the impress of vigorous variability occurring on a variety of spatial and temporal scales. It should be kept in mind, though, that because of the substantial decadal variability of the full-depth circulation in the region (see section 2), several-year mean circulation patterns obtained for different time spans may substantially differ from each other both quantitatively and qualitatively [e.g., *Våge et al.*, 2011, Figure 10].

[70] The methodological outcome of the present analysis is that the combined use of repeat hydrography, Rio05 MDT and satellite altimetry data can provide a useful estimate of the mean full-depth circulation across a transatlantic section without imposing a priori constraints.

[71] **Acknowledgments.** We thank all who contributed to the hydrographic and satellite data acquisition and processing. The editor and two anonymous reviewers are gratefully acknowledged for their constructive comments. The study was supported by the Russian Ministry of Education and Science under the "World Ocean" Federal Programme (contract 01.420.1.2.0001), the RFBR grants 10-05-00029, 11-05-00555 and 12-05-91056-CNRS, and the Russian President grants MK-394.2010.5 and MK-1636.2011.5. H. Mercier and C. Gourcuff are supported by the French National Center for Scientific Research (CNRS), P. Lherminier and F. Gaillard by the French Institute for Marine Science (Ifremer) and N. Daniault by the European University of Brittany.

References

Bacon, S. (1997), Circulation and fluxes in the North Atlantic between Greenland and Ireland, *J. Phys. Oceanogr.*, *27*, 1420–1435, doi:10.1175/1520-0485(1997)027<1420:CAFITN>2.0.CO;2.

Bacon, S. (1998), Decadal variability in the outflow from the Nordic Seas to the deep Atlantic Ocean, *Nature*, *394*, 871–874, doi:10.1038/29736.

Bacon, S., and P. Saunders (2010), The deep western boundary current at Cape Farewell: Results from a moored current meter array, *J. Phys. Oceanogr.*, *40*, 815–829, doi:10.1175/ 2009JPO4091.1.

Baudrillard, J. (1988), Simulacra and simulations, in *Jean Baudrillard, Selected Writings*, edited by M. Poster, pp. 166–184, Stanford Univ. Press, Stanford, Calif.

Bersch, M. (1995), On the circulation of the northeastern North Atlantic, *Deep Sea Res., Part I*, *42*, 1583–1607, doi:10.1016/0967-0637(95)00071-D.

Bersch, M., I. Yashayaev, and K. P. Koltermann (2007), Recent changes of the thermohaline circulation in the subpolar North Atlantic, *Ocean Dyn.*, *57*, 223–235, doi:10.1007/s10236-007-0104-7.

Bower, A. S., M. S. Lozier, S. F. Gary, and C. W. Böning (2009), Interior pathways of the North Atlantic Meridional Overturning Circulation, *Nature*, *459*, 243–247, doi:10.1038/nature07979.

Clarke, R. A. (1984), Transport through the Cape Farewell–Flemish Cap section, *Rapp. P.-V. Reun.- Cons. Int. Explor. Mer*, *185*, 120–130.

Cunningham, S., et al. (2009), The present and future system for measuring the Atlantic meridional overturning circulation and heat transport, paper presented at OceanObs'09: Sustained Ocean Observations and Information for Society, Eur. Space Agency,Venice, Italy, 21–25 Sep.

Daniault, N., P. Lherminier, and H. Mercier (2011a), Circulation and transport at the south east tip of Greenland, *J. Phys. Oceanogr.*, *41*, 437–457, doi:10.1175/2010JPO4428.1.

Daniault, N., H. Mercier, and P. Lherminier (2011b), The 1992–2009 transport variability of the East Greenland–Irminger Current at 60°N, *Geophys. Res. Lett.*, *38*, L07601, doi:10.1029/2011GL046863.

Dengler, M., J. Fischer, F. A. Schott, and R. Zantopp (2006), Deep Labrador Current and its variability in 1996–2005, *Geophys. Res. Lett.*, *33*, L21S06, doi:10.1029/2006GL026702.

Dickson, R. R., and J. Brown (1994), The production of North Atlantic Deep Water: Sources, rates and pathways, *J. Geophys. Res.*, *99*(C6), 12,319–12,341, doi:10.1029/94JC00530.

Dickson, R., et al. (2008), The overflow flux west of Iceland: Variability, origins and forcing, in *Arctic–Subarctic Ocean Fluxes*, edited by R. Dickson, J. Meincke, and P. Rhines, pp. 443–474, Springer, New York, doi:10.1007/978-1-4020-6774-7_20.

Falina, A., A. Sarafanov, and A. Sokov (2007), Variability and renewal of Labrador Sea Water in the Irminger Basin in 1991–2004, *J. Geophys. Res.*, *112*, C01006, doi:10.1029/2005JC003348.

Fischer, J., M. Visbeck, R. Zantopp, and N. Nunes (2010), Interannual to decadal variability of outflow from the Labrador Sea, *Geophys. Res. Lett.*, *37*, L24610, doi:10.1029/2010GL045321.

Garzoli, S. L., et al. (2009), Progressing towards global sustained deep ocean observations, paper presented at OceanObs'09: Sustained Ocean Observations and Information for Society, Eur. Space Agency, Venice, Italy, 21–25 Sep.

Gourcuff, C. (2008), Etude de la variabilité de la circulation du gyre subpolaire de l'Atlantique Nord à partir des données Ovide et de mesures satellitaires, PhD thesis, Univ. de Bretagne Occident., Brest, France. [Available at http://archimer.ifremer.fr/doc/00000/6226/.]

Gourcuff, C., P. Lherminier, H. Mercier, and P. Y. Le Traon (2011), Altimetry combined with hydrography for ocean transport estimation, *J. Atmos. Oceanic Technol.*, *28*, 1324–1337,doi:10.1175/2011JTECHO818.1.

Häkkinen, S., and P. B. Rhines (2004), Decline of subpolar North Atlantic circulation during the 1990s, *Science*, *304*, 555–559, doi:10.1126/science.1094917.

Häkkinen, S., and P. B. Rhines (2009), Shifting surface currents in the northern North Atlantic Ocean, *J. Geophys. Res.*, *114*, C04005, doi:10.1029/2008JC004883.

Hansen, B., and S. Østerhus (2007), Faroe Bank Channel overflow 1995–2005, *Prog. Oceanogr.*, *75*, 817–856, doi:10.1016/j.pocean.2007.09.004.

Hansen, B., H. Hátún, R. Kristiansen, S. M. Olsen, and S. Østerhus (2010), Stability and forcing of the Iceland-Faroe inflow of water, heat, and salt to the Arctic, *Ocean Sci.*, *6*, 1013–1026, doi:10.5194/os-6-1013-2010.

Hátún, H., A. B. Sandø, and H. Drange (2005), Influence of the Atlantic Subpolar Gyre on the thermohaline circulation, *Science*, *309*, 1841–1844, doi:10.1126/science.1114777.

Holliday, N. P., S. Bacon, J. Allen, and E. L. McDonagh (2009), Circulation and transport in the western boundary currents at Cape Farewell, Greenland, *J. Phys. Oceanogr.*, *39*, 1854–1870, doi:10.1175/2009JPO4160.1.

Hurrell, J. W. (1995), Decadal trends in the North Atlantic Oscillation: Regional temperatures and precipitation, *Science*, *269*, 676–679, doi:10.1126/science.269.5224.676.

Koltermann, K. P., A. Sokov, V. Tereschencov, S. Dobroliubov, K. Lorbacher, and A. Sy (1999), Decadal changes in the thermohaline circulation of the North Atlantic, *Deep Sea Res., Part II*, *46*, 109–138, doi:10.1016/S0967-0645(98)00115-5.

Lazier, J., R. Hendry, A. Clarke, I. Yashayaev, and P. Rhines (2002), Convection and restratification in the Labrador Sea, 1990–2000, *Deep Sea Res., Part I*, *49*, 1819–1835, doi:10.1016/S0967-0637(02)00064-X.

Lherminier, P., H. Mercier, C. Gourcuff, M. Alvarez, S. Bacon, and C. Kermabon (2007), Transports across the 2002 Greenland-Portugal Ovide section and comparison with 1997, *J. Geophys. Res.*, *112*, C07003, doi:10.1029/2006JC003716.

Lherminier, P., H. Mercier, T. Huck, C. Gourcuff, F. F. Perez, P. Morin, A. Sarafanov, and A. Falina (2010), The Atlantic Meridional Overturning Circulation and the subpolar gyre observed at the A25-Ovide section in June 2002 and 2004, *Deep-Sea Res., Part I*, *57*, 1374–1391, doi:10.1016/j.dsr.2010.07.009.

Lozier, M. S., and N. M. Stewart (2008), On the temporally varying northward penetration of Mediterranean Overflow Water and eastward penetration of

Labrador Sea Water, *J. Phys. Oceanogr.*, *38*, 2097–2103, doi:10.1175/2008JPO3908.1.

Lumpkin, R., and K. Speer (2007), Global ocean meridional overturning, *J. Phys. Oceanogr.*, *37*, 2550–2562, doi:10.1175/JPO3130.1.

Lumpkin, R., K. G. Speer, and K. P. Koltermann (2008), Transport across 48°N in the Atlantic Ocean, *J. Phys. Oceanogr.*, *38*, 733–752, doi:10.1175/2007JPO3636.1.

Macrander, A., U. Send, H. Valdimarsson, S. Jónsson, and R. H. Käse (2005), Interannual changes in the overflow from the Nordic Seas into the Atlantic Ocean through Denmark Strait, *Geophys. Res. Lett.*, *32*, L06606, doi:10.1029/2004GL021463.

McCartney, M. S., and L. D. Talley (1982), The Subpolar Mode Water of the North Atlantic Ocean, *J. Phys. Oceanogr.*, *12*, 1169–1188, doi:10.1175/1520-0485(1982)012<1169:TSMWOT>2.0.CO;2.

Mork, K. A., and Ø. Skagseth (2010), A quantitative description of the Norwegian Atlantic Current by combining altimetry and hydrography, *Ocean Sci.*, *6*, 901–911, doi:10.5194/os-6-901-2010.

Olsen, S. M., B. Hansen, D. Quadfasel, and S. Østerhus (2008), Observed and modelled stability of overflow across the Greenland-Scotland Ridge, *Nature*, *455*, 519–522, doi:10.1038/nature07302.

Østerhus, S., W. R. Turrell, S. Jónsson, and B. Hansen (2005), Measured volume, heat, and salt fluxes from the Atlantic to the Arctic Mediterranean, *Geophys. Res. Lett.*, *32*, L07603, doi:10.1029/2004GL022188.

Østerhus, S., T. Sherwin, D. Quadfasel, and B. Hansen (2008), The overflow transport east of Iceland, in *Arctic–Subarctic Ocean Fluxes*, edited by R. Dickson, J. Meincke, and P. Rhines, pp. 427–441, Springer, New York, doi:10.1007/978-1-4020-6774-7_19.

Pickart, R. S., and M. A. Spall (2007), Impact of Labrador Sea convection on the North Atlantic Meridional Overturning Circulation, *J. Phys. Oceanogr.*, *37*, 2207–2227, doi:10.1175/JPO3178.1.

Pickart, R. S., F. Straneo, and G. W. K. Moore (2003), Is Labrador Sea Water formed in the Irminger Basin?, *Deep Sea Res., Part I*, *50*, 23–52, doi:10.1016/S0967-0637(02)00134-6.

Rhein, M., D. Kieke, S. Hüttl-Kabus, A. Roessler, C. Mertens, R. Meissner, B. Klein, C. W. Böning, and I. Yashayaev (2011), Deep-water formation, the subpolar gyre, and the meridional overturning circulation in the subpolar North Atlantic, *Deep Sea Res., Part II*, *58*, 1819–1832, doi:10.1016/j.dsr2.2010.10.061.

Rio, M.-H., and F. Hernandez (2004), A mean dynamic topography computed over the world ocean from altimetry, in situ measurements, and a geoid model, *J. Geophys. Res.*, *109*, C12032, doi:10.1029/2003JC002226.

Sarafanov, A., A. Sokov, A. Demidov, and A. Falina (2007), Warming and salinification of intermediate and deep waters in the Irminger Sea and Iceland Basin in 1997–2006, *Geophys. Res. Lett.*, *34*, L23609, doi:10.1029/2007GL031074.

Sarafanov, A., A. Falina, A. Sokov, and A. Demidov (2008), Intense warming and salinification of intermediate waters of southern origin in the eastern subpolar North Atlantic in the 1990s to mid-2000s, *J. Geophys. Res.*, *113*, C12022, doi:10.1029/2008JC004975.

Sarafanov, A., A. Falina, H. Mercier, P. Lherminier, and A. Sokov (2009), Recent changes in the Greenland–Scotland overflow-derived water transport inferred from hydrographic observations in the southern Irminger Sea, *Geophys. Res. Lett.*, *36*, L13606, doi:10.1029/2009GL038385.

Sarafanov, A., A. Falina, P. Lherminier, H. Mercier, A. Sokov, and C. Gourcuff (2010), Assessing decadal changes in the Deep Western Boundary Current absolute transport southeast of Cape Farewell (Greenland) from hydrography and altimetry, *J. Geophys. Res.*, *115*, C11003, doi:10.1029/2009JC005811.

Saunders, P. M. (1994), The flux of overflow water through the Charlie-Gibbs Fracture Zone, *J. Geophys. Res.*, *99*, 12,343–12,355, doi:10.1029/94JC00527.

Saunders, P. M. (1996), The flux of dense cold overflow water southeast of Iceland, *J. Phys. Oceanogr.*, *26*, 85–95, doi:10.1175/1520-0485(1996)026<0085:TFODCO>2.0.CO;2.

Schmitz, W. J., Jr., and M. S. McCartney (1993), On the North Atlantic Circulation, *Rev. Geophys.*, *31*, 29–49, doi:10.1029/92RG02583.

Schott, F. A., and P. Brandt (2007), Circulation and deep water export of the subpolar North Atlantic during the 1990s, in *Ocean Circulation: Mechanisms and Impacts*, *Geophys. Monogr. Ser.*, vol. 173, edited by A. Schmittner, J. Chiang, and S. Hemmings, pp. 91–118, AGU, Washington, D. C., doi:10.1029/173GM08.

Sutherland, D. A., and R. S. Pickart (2008), The East Greenland Coastal Current: Structure, variability, and forcing, *Prog. Oceanogr.*, *78*, 58–77, doi:10.1016/j.pocean.2007.09.006.

Talley, L. D., and M. S. McCartney (1982), Distribution and circulation of Labrador Sea water, *J. Phys. Oceanogr.*, *12*, 1189–1205, doi:10.1175/1520-0485(1982)012<1189:DACOLS>2.0.CO;2.

Thierry, V., E. de Boisséson, and H. Mercier (2008), Interannual variability of the Subpolar Mode Water properties over the Reykjanes Ridge during 1990–2006, *J. Geophys. Res.*, *113*, C04016, doi:10.1029/2007JC004443.

Våge, K., R. S. Pickart, V. Thierry, G. Reverdin, C. M. Lee, B. Petrie, T. A. Agnew, A. Wong, and M. H. Ribergaard (2009), Surprising return of deep convection to the subpolar North Atlantic Ocean in winter 2007–2008, *Nat. Geosci.*, *2*, 67–72, doi:10.1038/ngeo382.

Våge, K., R. Pickart, A. Sarafanov, Ø. Knutsen, H. Mercier, P. Lherminier, H. van Aken, J. Meincke, D. Quadfasel, and S. Bacon (2011), The Irminger Gyre: Circulation, convection, and interannual variability, *Deep Sea Res., Part I*, *58*, 590–614, doi:10.1016/j.dsr.2011.03.001.

van Aken, H. M., M. F. de Jong, and I. Yashayaev (2011), Decadal and multi-decadal variability of Labrador Sea Water in the north–western North Atlantic Ocean derived from tracer distributions: Heat budget, ventilation, and advection, *Deep-Sea Res., Part I*, *58*, 505–523, doi:10.1016/j.dsr.2011.02.008.

Willis, J. K. (2010), Can in situ floats and satellite altimeters detect long-term changes in Atlantic Ocean overturning?, *Geophys. Res. Lett.*, *37*, L06602, doi:10.1029/2010GL042372.

Xu, X., W. J. Schmitz Jr., H. E. Hurlburt, P. J. Hogan, and E. P. Chassignet (2010), Transport of Nordic Seas overflow water into and within the Irminger Sea: An eddy-resolving simulation and observations, *J. Geophys. Res.*, *115*, C12048, doi:10.1029/2010JC006351.

Yashayaev, I. (2007), Hydrographic changes in the Labrador Sea, 1960–2005, *Prog. Oceanogr.*, *73*, 242–276, doi:10.1016/j.pocean.2007.04.015.

Yashayaev, I., H. M. van Aken, N. P. Holliday, and M. Bersch (2007), Transformation of the Labrador Sea Water in the subpolar North Atlantic, *Geophys. Res. Lett.*, *34*, L22605, doi:10.1029/2007GL031812.

N. Daniault, Laboratoire de Physique des Océans, UMR 6523, UBO, CNRS/Ifremer/IRD, 6 Ave. Le Gorgeu, CS 93837, Brest F-29238, France.

A. Falina, S. Gladyshev, A. Sarafanov, and A. Sokov, P.P. Shirshov Institute of Oceanology, 36, Nakhimovskiy Prospect, 117997 Moscow, Russia. (sarafanov@mail.ru)

F. Gaillard, C. Gourcuff, P. Lherminier, and H. Mercier, Laboratoire de Physique des Océans, UMR 6523, IFREMER, CNRS/IRD/UBO, BP 70, Plouzane F-29280, France.